AFRL-RX-WP-TR-2011-4046

DURABLE HYBRID COATINGS

Vsevold Balbyshev, Larry R. Pederson, Dante Battocchi, and Gordon P. Bierwagen

North Dakota State University

JANUARY 2010
Interim Report

AIR FORCE RESEARCH LABORATORY
MATERIALS AND MANUFACTURING DIRECTORATE
WRIGHT-PATTERSON AIR FORCE BASE, OH 45433-7750
AIR FORCE MATERIEL COMMAND
UNITED STATES AIR FORCE

NOTICE AND SIGNATURE PAGE

Using Government drawings, specifications, or other data included in this document for any purpose other than Government procurement does not in any way obligate the U.S. Government. The fact that the Government formulated or supplied the drawings, specifications, or other data does not license the holder or any other person or corporation; or convey any rights or permission to manufacture, use, or sell any patented invention that may relate to them.

This report was cleared for public release by the Wright-Patterson Public Affairs Office and is available to the general public, including foreign nationals. Copies may be obtained from the Defense Technical Information Center (DTIC) (http://www.dtic.mil).

AFRL-RX-WP-TR-2011-4046 HAS BEEN REVIEWED AND IS APPROVED FOR PUBLICATION IN ACCORDANCE WITH ASSIGNED DISTRIBUTION STATEMENT.

*//signature//

AARON VEYDT, Program Manager
Thermal Sciences and Materials Branch
Nonmetallic Materials Division

*//signature//

NADER HENDIZADEH, Chief
Thermal Sciences and Materials Branch
Nonmetallic Materials Division

*//signature//

SHASHI K. SHARMA, Deputy Chief
Nonmetallic Materials Division
Materials and Manufacturing Directorate

This report is published in the interest of scientific and technical information exchange, and its publication does not constitute the Government's approval or disapproval of its ideas or findings.

*Disseminated copies will show "//signature//" stamped or typed above the signature blocks.

REPORT DOCUMENTATION PAGE

Form Approved
OMB No. 0704-0188

1. REPORT DATE *(DD-MM-YY)*	2. REPORT TYPE	3. DATES COVERED *(From - To)*
January 2011	Interim	01 October 2009 – 30 September 2010

4. TITLE AND SUBTITLE
DURABLE HYBRID COATINGS

5a. CONTRACT NUMBER
FA8650-04-1-5045

5b. GRANT NUMBER

5c. PROGRAM ELEMENT NUMBER
62102F

6. AUTHOR(S)
Vsevold Balbyshev, Larry R. Pederson, Dante Battocchi, and Gordon P. Bierwagen

5d. PROJECT NUMBER
4347

5e. TASK NUMBER
30

5f. WORK UNIT NUMBER
65100002

7. PERFORMING ORGANIZATION NAME(S) AND ADDRESS(ES)
North Dakota State University
1805 NDSU Research Park Drive N
Fargo, ND 58102

8. PERFORMING ORGANIZATION REPORT NUMBER

9. SPONSORING/MONITORING AGENCY NAME(S) AND ADDRESS(ES)
Air Force Research Laboratory
Materials and Manufacturing Directorate
Wright-Patterson Air Force Base, OH 45433-7750
Air Force Materiel Command
United States Air Force

10. SPONSORING/MONITORING AGENCY ACRONYM(S)
AFRL/RXBT

11. SPONSORING/MONITORING AGENCY REPORT NUMBER(S)
AFRL-RX-WP-TR-2011-4046

12. DISTRIBUTION/AVAILABILITY STATEMENT
Approved for public release; distribution unlimited.

13. SUPPLEMENTARY NOTES
PAO case number 88ABW-2011-2400, cleared 29 April 2011. Report contains color.

14. ABSTRACT
A new *in situ* corrosion sensor electrode was designed, fabricated, and tested. The new sensor was shown in performance testing to be robust, flexible, reproducible, and adaptable to various field applications. The shape and size of the sensor could be easily changed by creating the appropriate shadow mask for metal deposition. Sensors were embedded between a Mg-rich primer, developed earlier with support from this project, and the topcoat. Coated substrates with embedded sensors were then placed into a standardized Prohesion chamber to simulate weathering conditions in an aggressive manner to induce accelerated coating failure. It was demonstrated that the embedded sensors enabled continuous monitoring of degradation of the coating system with Prohesion exposure time, through a gradual decrease in both the low frequency impedance |Z|0.05 Hz and noise resistance. Further, the 2-electode sensor-sensor electrochemical impedance data agreed well with the data obtained from the conventional 3-electrode setup performed in a laboratory environment, thus demonstrating the feasibility of this 2 sensor electrode approach without the need of additional reference or counter electrodes.

15. SUBJECT TERMS
high-throughput (HT), embedded sensor, in situ monitoring, Mg-rich primer

16. SECURITY CLASSIFICATION OF:			17. LIMITATION OF ABSTRACT:	18. NUMBER OF PAGES	19a. NAME OF RESPONSIBLE PERSON (Monitor)
a. REPORT	b. ABSTRACT	c. THIS PAGE			Aaron Veydt
Unclassified	Unclassified	Unclassified	SAR	66	19b. TELEPHONE NUMBER *(Include Area Code)* N/A

Standard Form 298 (Rev. 8-98)
Prescribed by ANSI Std. Z39-18

Table of Contents

List of Figures

List of Tables

Acknowledgements

This material is based on research sponsored by Air Force Research Laboratory under agreement number FA8650-04-1-5045.

The views and conclusions contained herein are those of the authors and should not be interpreted as necessarily representing the official policies or endorsements, either expressed or implied, of Air Force Research Laboratory or the U.S. Government.

Distribution List

Air Force Research Laboratory

AFRL/MLBT: Aaron R. Veydt, 1Lt, USAF — 1 e-mail copy: Aaron.Veydt@wpafb.af.mil
Copy to: Dr. Stephen L. Szaruga — 1 e-mail copy; Steve.Szaruga@wpafb.af.mil
2941 P. Street, Rm 136
Wright-Patterson Air Force Base, Ohio 45433-7750

AFR/PKMM:L: Michael A. Cramer — 1 e-mail copy: Michael.Cramer@wpafb.af.mil
Copy to: Rebecca Powers — 1 e-mail copy: Rebecca.Powers@wpafb.af.mil

Office of Naval Research – Administrative Grants Officer

Sandra Thomson — 1 e-mail copy: Sandra.Thomson@navy.mil
ONR Seattle Regional Office
1107 NE45th Street, Suite 350
Seattle WA 98105-4631

North Dakota State University

Dr. Gordon Bierwagen — 1 e-mail copy: Gordon.Bierwagen@ndsu.edu
Dr. Séva Balbyshev — 1 e-mail copy: Seva.Balbyshev@ndsu.edu
Dr. Eng. Dante Battocchi — 1 e-mail copy: Dante.Battocci@ndsu.edu
Mr. Aaron Reinholz — 1 e-mail copy: Aaron.Reinholz@ndsu.edu
Dr. Philip Boudjouk — 1 e-mail copy: Philip.Boudjouk@ndsu.edu

Contact Information for Inquiries

Programmatic:
Larry Pederson, Director CNSE
1805 NDSU Research Park Dr. N.
Fargo, ND 58102
(701) 231-5284 (voice)
(701) 231-7916 (fax)
Larry.Pederson@ndsu.edu

Technical:
Gordon Bierwagen, Professor
Department of Coatings & Polymeric Materials
1735 NDSU Research Park Dr. N.
Fargo, ND 58102
(701) 231-8294 (voice) (701) 231-8439 (fax)
Gordon.Bierwagen@ndsu.edu

Financial:
Mark Lande, Asst. Dir. CNSE
Admin. and Financial Services
1805 NDSU Research Park Dr.
Fargo, ND 58102
(701) 231-5882 (voice)
(701) 231-7916 (fax)
Mark.Lande@ndsu.edu

Summary

The overall goal of this project is to contribute to the development of the next-generation anti-corrosion and other protective coating systems for USAF aircraft. During the past year, NDSU focused on the development and testing of embedded electrochemical sensors for magnesium-rich primers. Unlike conventional electrochemical sensors that monitor the metal substrate itself and provide no information about the coating, the NDSU *in situ* corrosion sensors are embedded between the primer and the topcoat and thus are suitable for monitoring the corrosion protection afforded by the metal-rich primer. Further, the embedded sensors are shielded from the environment by the topcoat, which prolongs the electrode life as well as reduces the noise associated with measurements.

To that end, a new *in situ* corrosion sensor electrode was designed, fabricated, and tested. The new sensor was shown in performance testing to be robust, flexible, reproducible, and adaptable to various field applications. The shape and size of the sensor could be easily changed by creating the appropriate shadow mask for metal deposition. Sensors were embedded between a Mg-rich primer, which was developed earlier with support from this project, and the topcoat. Coated substrates with embedded sensors were then placed into a standardized Prohesion® chamber to simulate weathering conditions in an aggressive manner to induce accelerated coating failure. It was demonstrated that the embedded sensors enabled continuous monitoring of degradation of the coating system with Prohesion® exposure time, through a gradual decrease in both the low frequency impedance $|Z|_{0.05\ Hz}$ and noise resistance. Further, the 2-electode Sensor-Sensor electrochemical impedance data agreed well with the data obtained from the conventional 3-electrode setup performed in a laboratory environment, thus demonstrating the feasibility of this 2 sensor electrode approach without the need of additional reference or counter electrodes.

1.0 Introduction

The overall goal of this program conducted at North Dakota State University (NDSU) is to contribute to the development of the next-generation anti-corrosion and other protective coating systems for USAF aircraft. Technical progress during the past year focused on the development of coating prognostics, involving the use of embedded sensors to evaluate the effectiveness of previously-developed magnesium-based primers. Research on other topics, including Mg-rich primer development, high-throughput experimentation of coatings formulation and optimization, and plasma deposition of inorganic coatings, has been completed and progress described in prior years.

Aluminum alloys, especially AA2024-T3, are widely used in the aerospace industry because of their high strength and stiffness combined with low density. However, Al alloys are very sensitive to corrosion environments due to their high copper content. Recently developed metal-rich coatings for corrosion protection of aircraft aluminum alloys rely on magnesium powder dispersed in an organic binder. In these metal-rich coatings, Mg particles embedded in a polymeric matrix act as a sacrificial anode: Mg undergoes anodic dissolution and thus protects the underlying metal from corrosion. By analogy to zinc-rich primer coatings that keep steel from corrosion through cathodic protection, the Mg-rich primer (MRP) coatings, were designed, examined and developed by M. E. Nanna, D. Battocchi and G. P. Bierwagen at NDSU [Nanna and Bierwagen 2004; Bierwagen et al. 2005].

During the past year, the primary emphasis of this project has been focused on the development of wireless corrosion sensors for monitoring cathodic protection of metal-rich primers, such as those developed for the protection of aircraft aluminum alloys. Recently, there has been extensive development of several in situ sensing techniques that monitor the barrier properties of a coating. Most research in electrochemical sensors has been focused on sensor electrodes embedded in the substrate. Such sensors monitor corrosion of the metal substrate but provide no information about the film itself. Thus, they are unsuitable for monitoring corrosion within the metal-rich primer itself. A new technique for in situ monitoring of a coating with ac involves the application of an embedded electrode or sensor within the coating. The Department of Coatings and Polymeric Materials (CPM) and Center for Nanoscale Science and Engineering (CNSE) at NDSU have been at the forefront in the development, feasibility demonstration, and application of embedded sensors, which consist of electrodes that act as the counter and reference but are placed between the layers of two-layered coating systems. An advantage of the embedded electrodes is that they are shielded from the environment by the topcoat, which prolongs the electrode life as well as reduces the noise associated with measurements. Another advantage is that

electrochemical measurement of the primer and primer/metal interface can be made without being masked by high resistant topcoats. The coupling of embedded sensors and coating systems with Mg-rich primers is a unique approach that allows in situ monitoring of the electrochemical behavior of protective Mg-rich primers beneath a topcoat.

This report describes the development of embedded sensor electrode technology, and the application of this new sensor in *in situ* monitoring of the Mg-rich primer beneath a topcoat in a salt fog and under Prohesion® conditions. Concepts for development of remote health monitoring of structural parts, remote areas, and difficult to reach spaces are additionally discussed. The new corrosion sensor was demonstrated to be robust, yield reproducible results, and adaptable to a wide range of field conditions.

2.0 Coating Prognostics

In this task, NDSU investigated the application of embedded electrochemical sensors for magnesium-rich primers. Unlike conventional electrochemical sensors that monitor the metal substrate itself and provide no information about the coating, the NDSU *in situ* corrosion sensors are embedded between the primer and the topcoat and thus are suitable for monitoring the corrosion protection afforded by the metal-rich primer. As an added advantage, the embedded sensor electrodes are shielded from the environment by the topcoat, which prolongs the electrode life as well as reduces the noise associated with measurements. Moreover, electrochemical measurements of the primer and primer/metal interface can be carried out without being masked by high resistant topcoats.

2.1 Embedded Sensor Electrode Development

The embedded sensor electrode developed at NDSU is part of the effort aimed at development of wireless corrosion sensors for monitoring cathodic protection of metal-rich primers. Such electrodes are robust and reproducible, while at the same time being thin, flexible, and adaptable to various field applications. Sensor electrodes were made by the industry standard selective laser etching procedure utilized by many common printed circuit board manufacturers. The shape and size of the sensor can be easily changed by creating the appropriate shadow mask for metal deposition.

Initially, sensor electrodes were arranged in pairs as shown in Figure 1. The conductive "finger" represented the sensing area of the electrodes. The spacing between the "fingers" could be varied. In Figure 1, the inter-digital spacing is 1000 μm and 500 μm for the top and bottom designs respectively. Such an inter-digitated design is conducive to monitoring of electrolyte ingress through the topcoat to the primer/topcoat interface and can provide additional insight into the onset of coating degradation in corrosive environment. However, for *primer-only* sensing, the "fingers" are not required in most applications.

This information provided guidance for the development of a more streamlined sensor electrode, based on the same manufacturing approach of magnetron sputtering of metal on Kapton® film. Magnetron sputtering is a form physical vapor deposition (PVD), in which a glow plasma discharge bombards a target. This results in the ejection of some material from the target, which then deposits onto a substrate.

The new generation of the sensor electrode is shown in Figure 2. The paddle-like sensors were designed in Design Capture/Expedition by Mentor Graphics (Mentor Graphics, Wilsonville, OR).

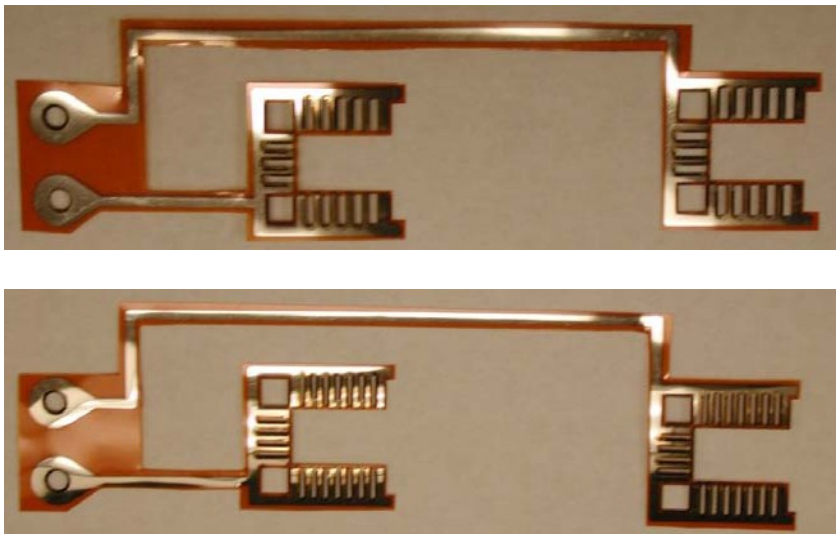

Figure 1. Sensor arrays of an interdigitated design.

Figure 2. New generation platinum (top) and aluminum (bottom) sensor electrodes.

In the next step, the inverted image of the sensor generated by computer-assisted design (CAD) software was used to manufacture a shadow mask (stencil) for subsequent magnetron sputter deposition of metallic film (conductive path of a sensor). The shadow mask, shown in Figure 3, was made from series 316 stainless steel by Great Lakes Engineering (Maple Grove, MN). The deposition step was performed at NDSU CNSE on a Model CMS-18 PVD sputtering system (Kurt J. Lesker Company, Clairton, PA). For better adhesion, a 50 Å layer of Cr (99.95% pure, from Kurt J. Lesker Company, Clairton, PA) was first vapor deposited on a 2 mil thick Kapton® film (obtained from McMaster-Carr, Robbinsville, NJ),

followed by the deposition of 1500 Å layer of Pt (99.99% from Equipment Support Company USA Inc., Pensacola, FL), shown in Figure 2 (top). The sensors are not limited to the use of platinum or other expensive metals. However, selection of materials for the conductive aspect of the sensor must conform to the requirements of a particular application. The use of platinum was dictated by its superior conductivity at nanometer thicknesses and by the available of experimental electrochemical data for embedded sensors for Mg-rich primers.

The sensor electrode shown in Figure 2 (bottom) has a 2500 Å layer of aluminum on Kapton. The Al sensor can be used as a coupon electrode that monitor degradation of the primer and provides additional set of data in *in situ* corrosion experiments. The increased thickness of the Al electrode is dictated by its lower conductivity relative to Pt. Magnetron sputter deposition of Pt and Al electrodes of various shapes demonstrates the flexibility of the sensor manufacturing process at NDSU.

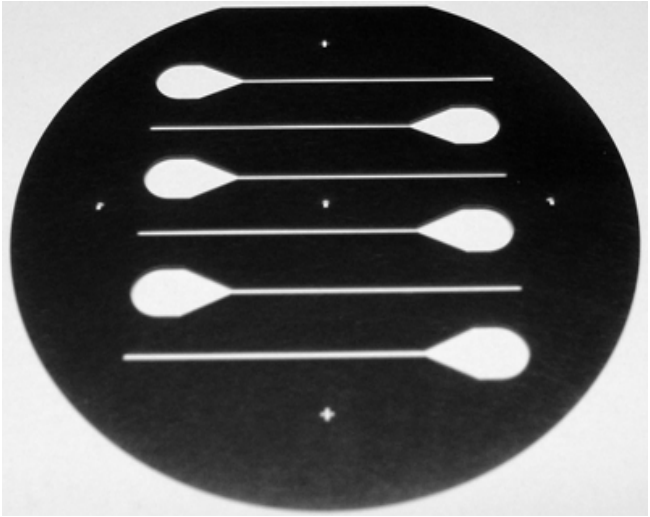

Figure 3. Stainless steel shadow mask, used to fabricate corrosion sensors by magnetron sputtering.

Following the deposition, the Kapton® pieces, 15 cm in diameter each as shown in Figure 4, were transferred to the Trumpf laser cutting station (Trumpf Inc, Farmington, CT). After the laser cutting step, excess Kapton® around the electrodes was removed, and the arrays were cleaned by ionized oxygen in March Plasma Treatment System (March Plasma Systems, Concord, CA), rubbed in isopropyl alcohol, and immersed in an ultrasonic bath. At this stage, the individual sensors were ready for deployment in corrosion testing.

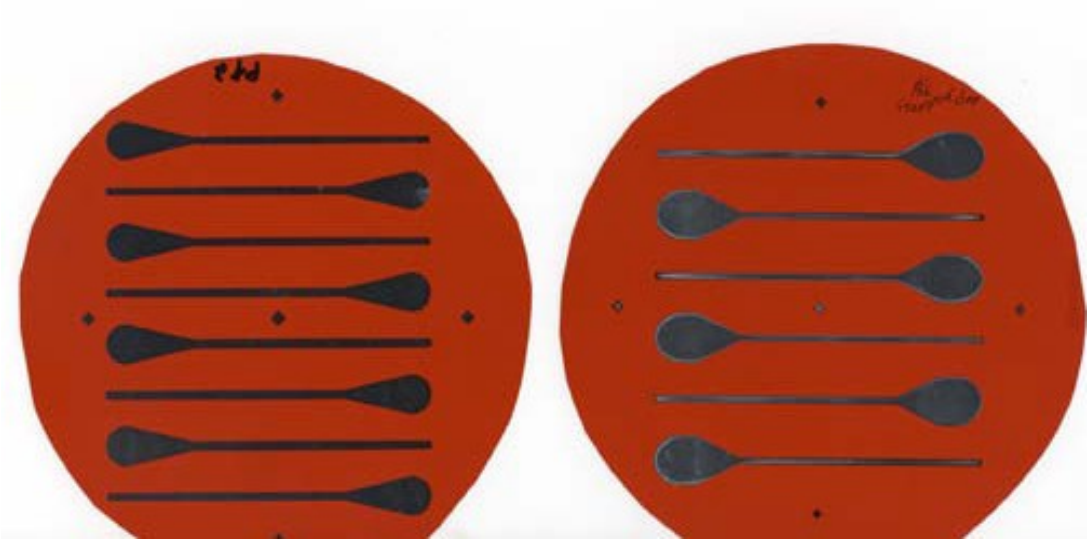

Figure 4. Kapton sheets with PVD deposited Pt (left) and Al (right). Laser cutting was utilized to separate individual sensors.

2.2. In Situ Monitoring of Mg-Rich Primer + Topcoat in B117 Chamber by Embedded Sensors

The protective coating system used in the experimental procedure was composed of a high solids polyurethane topcoat (Deft, Irvine, CA) and a Mg-rich primer developed at NDSU. In this primer, Mg powder with the average particle size of 25 μm (Ecka Granules of America, Louisville, KY) was dispersed in a two-component epoxy-polyamide resin, and the pigment volume concentration (PVC) of the primer was 45%. The primer was applied to a large 1' x 2' panel of aluminum alloy AA2024-T3. After the application of the primer, six platinum sensors were applied on the surface of the primer, followed by the application of the polyurethane topcoat.

The embedded sensors were placed between the primer and the topcoat at six different places. After curing, two scribes were made between sensors for comparison as shown in Figure 5 (spots 1 and 2). Two substrate contacts were present, shown in the upper corners of Figure 5. We used the most common corrosion resistance test method, American Society for Testing and Materials method ASTM-B117 - salt spray exposure, to investigate the corrosion performance of the coated panel by *in situ* monitoring its electrochemical properties with embedded sensors.

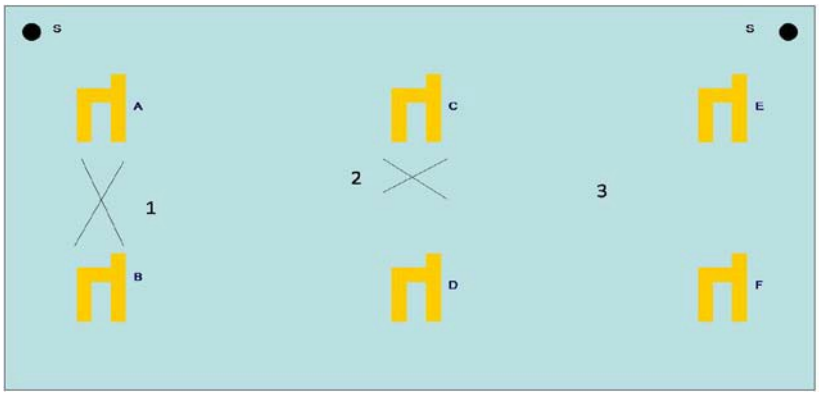

Figure 5. Sensors and scribes on aluminum alloy AA2024-T3 substrate.

Two-electrode (2E) electrochemical impedance spectroscopy (EIS) methods (either sensor-substrate or sensor-sensor) were used to evaluate corrosion processes. A total of 18 two-electrode EIS arrangements were tested each time for each panel, as specified in Table 1. In addition, control impedance spectra in a 3-electrode configuration (3E) were performed in three different areas for comparison (spots 1, 2 and 3 in Figure 5) with dilute Harrison's solution in the cells. Dilute Harrison's solution is an aqueous solution of 0.35 percent ammonium sulfate and 0.05 percent sodium chloride by weight, commonly used as the supporting electrolyte in tests with aluminum. In both sensor-substrate and sensor-sensor measurements in a two-electrode configuration, the final frequency was setup at 0.1 Hz, which was consistent with the sensor testing in the humidity chamber conducted in parallel. As for electrochemical noise measurements (ENM), a standard setup was followed, with 20 minutes per experiment duration for each combination. A total of 9 unique test arrangements were evaluated, as specified in Table 1. This protocol generates a sufficient amount of observations for data analysis. The details of EIS and ENM setups are described in Table 1, where "S" stands for substrates, and letters A through F represent sensor locations defined in Figure 5.

Table 1. Test Configurations in Electrochemical Impedance and Noise Measurements*

Electrochemical Impedance Spectroscopy (EIS) : (18 test arrangements)

2E: SA SB SC SD SE SF

AB AC AD BC BD CD CE CF EF

3E: ①②③

Control: Reference and Counter electrodes in positions 1, 2 and 3.

Electrochemical Noise Measurement (ENM): (9 test arrangements)

AB AC AD BC BD CD CE CF EF

*positions defined in Figure 5.

EIS and ENM were tested at 0, 1, 3, 7, 10 13, 17, 21, 24, 27, 30 and 34 days of B117 exposure. After the 34 days of B117 exposure, blisters appeared along the scribes, sensors and other areas on the surface of the panel. Thus, the coating had almost failed and tests were finished after 34 days of B117 exposure.

2.2.1 Electrochemical Impedance (EIS)

Figures 6 and 7 show the electrochemical impedance changes during the 34 days of B117 salt fog exposure. It can be observed that all three Bode plots display similar spectral features: at high frequency, the data overlap and are concentrated. But some data in the low-frequency range of the 2E sensor EIS were scattered, probably due to the harsh salt spray conditions, continuous changes of the coating surface and of the coating/substrate interface continuously. These phenomena also manifest themselves in the phase angle plot. The phase angle θ of the coating also gradually decreased with exposure duration. Its low frequency value was around 0° initially, and decreased down to -80-90° after 34 days of exposure, which indicated that the corrosion resistance of the coating system was substantially decreased.

The three-electrode EIS plot shown in Figure 8 appeared much smoother, as it was measured outside the chamber and under stable constant dilute Harrison's solution immersion. The phase angles, θ, of the 3E EIS were more stable and concentrated. The low-frequency phase angle value, θ, was around -60-65°, which was higher than its 2-electrode counterparts. As a whole, the EIS results showed that the *in situ* sensor-substrate testing monitored real-time changes of the coating interface and tracked the fluctuations of the salt spray chamber conditions, while the traditional 3E EIS was a static testing, reflecting an averaged and therefore more balanced and stable system.

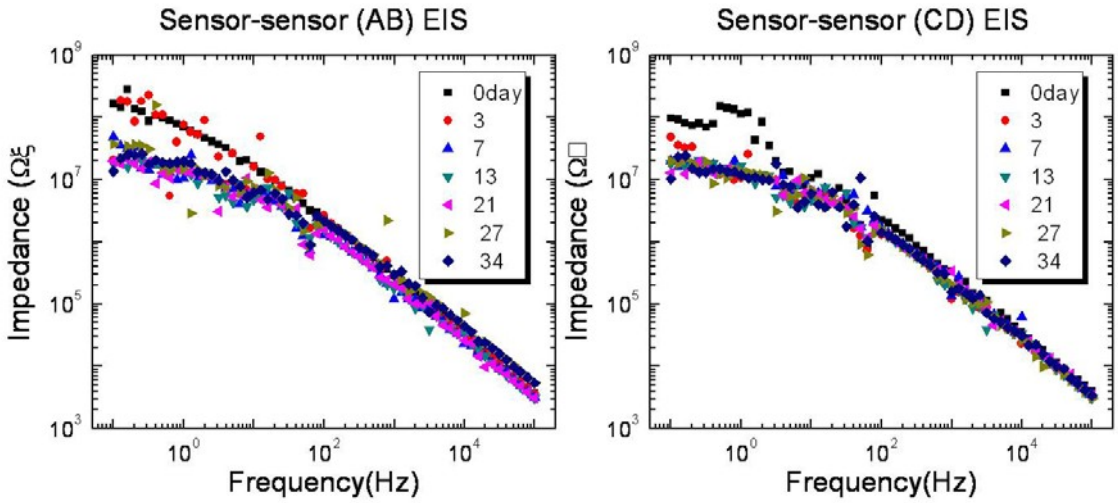

Figure 6. Bode plots of the sensor-sensor (AB and CD) obtained using 2-electrode EIS.

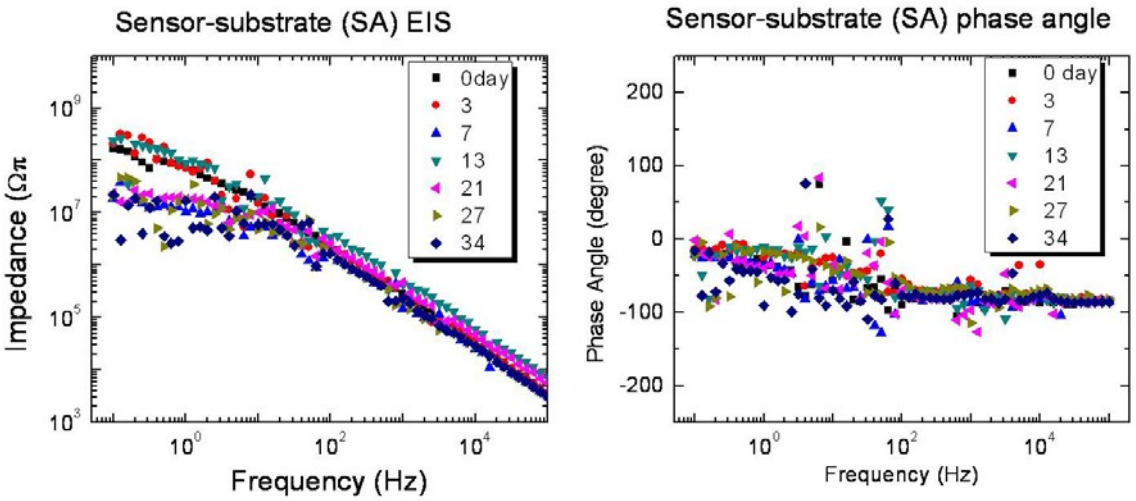

Figure 7. Bode and phase angle of the sensor-substrate (SA) obtained using 2-electrode EIS.

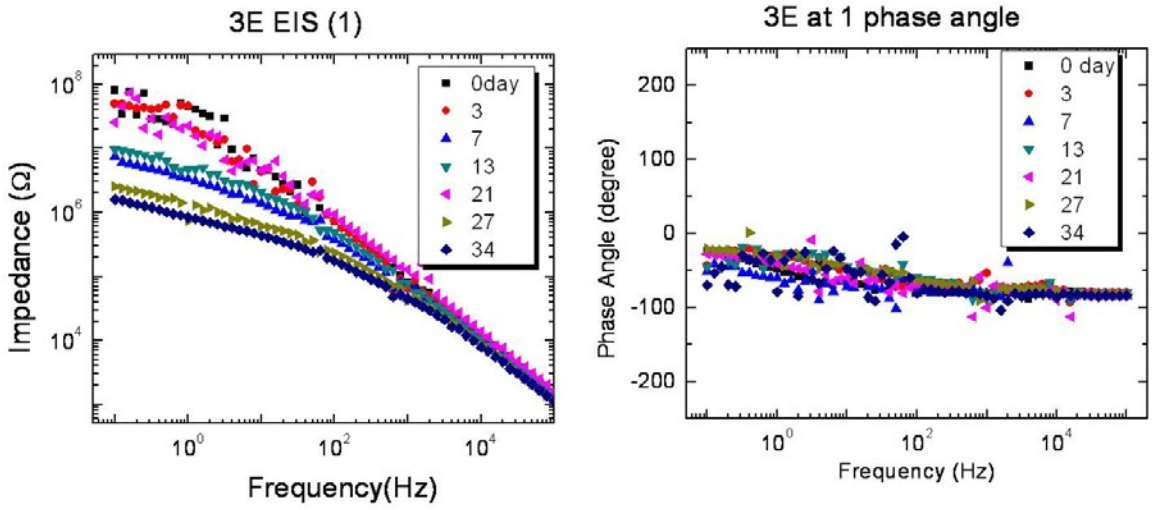

Figure 8. Bode and phase angle obtained using 3-electrode EIS at test area 1.

The additional difference between 2- and 3-electrode cell experiments can be seen in the magnitude of the low-frequency region, as shown in Figure 9. Here, the impedance values at the low-frequency limit, $|Z|_{0.1Hz}$, from the sensors were slightly higher and fluctuated more than the impedance values from the 3-electrode cell. But all $|Z|_{0.1Hz}$ values decreased with time from the initial high $10^{8}\,\Omega\,cm^{2}$ to $10^{6\text{-}7}\,\Omega\,cm^{2}$ after 34 days of B117 exposure, as expected. All the 2E data for substrate-sensor (SA, defined in Figure 5) and sensor-sensor (AB, defined in Figure 5) showed excellent dispersion throughout the entire B117 testing, which confirms the feasibility of *in situ* sensor monitoring of metal-rich primers.

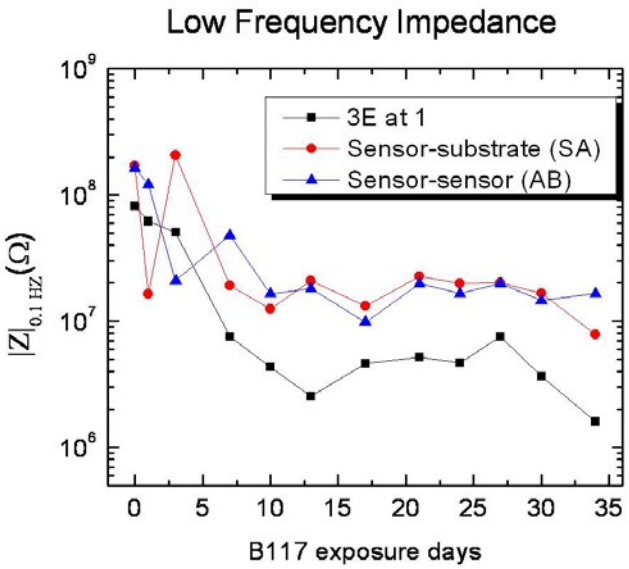

Figure 9. Three-electrode EIS at point 1 and low frequency impedance of positions SA and AB.

2.2.2 Open circuit potential (OCP)

The OCP of the coating system was tracked by 3E EIS measurements. Figure 10 shows the OCP changes at 3 different measuring areas, area 1 being close to the big scribe between sensor A and B, area 2 being next to the small scribe, and area 3 being relatively far from the sensors and the scribes (see Figure 5). The initial OCP (prior to B117 exposure) was not stable, since it needs a long electrolyte induction time. After exposure for just 1 day, the OCP dropped down to about -1.1 V and -1.3V (vs. SCE), corresponding to the magnesium particle activation; then increased with time and reached -0.8 V (vs. SCE) after 14 days of exposure, corresponding to the active magnesium pigment being gradually consumed (Figure 10). The OCP reached approximately -0.7 V (vs. SCE) after 25 days of B117 exposure and kept that value throughout the remainder of the test until failure occurred, indicating that cathodic protection of the Mg-rich primer had been weakened. The OCP values from 3 different areas were consistent with each other; they almost overlapped at the beginning and the end of the testing, but did show some variations in-between. From the OCP data, the *effective* cathodic protection time of the coating system was about 15 days (360 hrs) in B117 salt spray conditions.

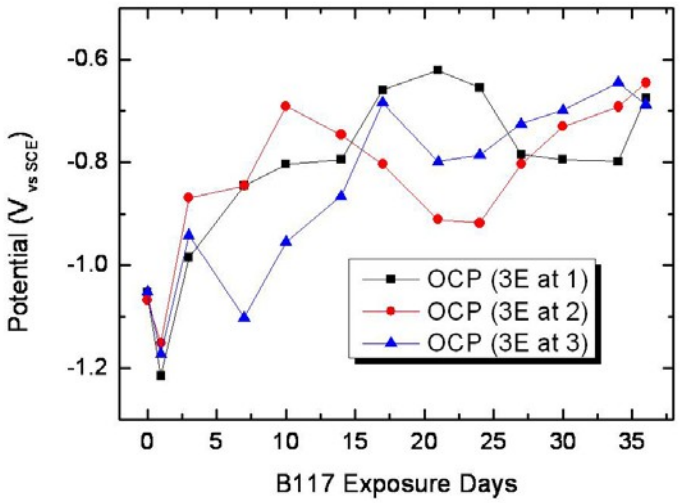

Figure 10. Open circuit potential changes, determined from 3-electrode EIS.

2.2.3 Electrochemical Noise Methods (ENM)

Electrochemical noise measurements were conducted while the two sensors were connected to the working and counter electrodes and the substrate was connected to the reference electrode. Both the electrochemical potential and current noise records were collected. The original ENM raw data are not reported here directly; instead, the noise resistance (R_n) value was obtained by dividing the standard deviation of potential noise by the standard deviation of current noise. The standard deviations of potential and current were calculated on small blocks of data of 256 points. Therefore, the R_n values reported here are, in turn, also average values over 256 data points.

Figure 11 shows the R_n changes between sensor A–B, and C–D, respectively. First, there was no obvious difference between R_n for A–B and R_n for C–D, where, there was a big scribe between A–B but only a small one between C–D. Therefore, it is difficult to estimate the size of the defects from the noise data alone. Second, the R_n data, as a whole, decreased gradually with exposure time, which was consistent with impedance results and tracked the coating property changes during the salt fog exposure. Finally, the absolute R_n values were almost an order of magnitude lower than the corresponding EIS $lZl_{0.1Hz}$ value. Most R_n values were located between 10^5 to 10^6 Ω. Both the impedance $|Z|_{0.1Hz}$ and noise R_n values showed that the corrosion resistance of the coating was gradually decreased with B117 exposure duration. But 2E EIS was more focused on the local sensor area monitoring, while the ENM reflected the averaging property between two sensors. So the EIS was locally more sensitive in picking up interfacial changes.

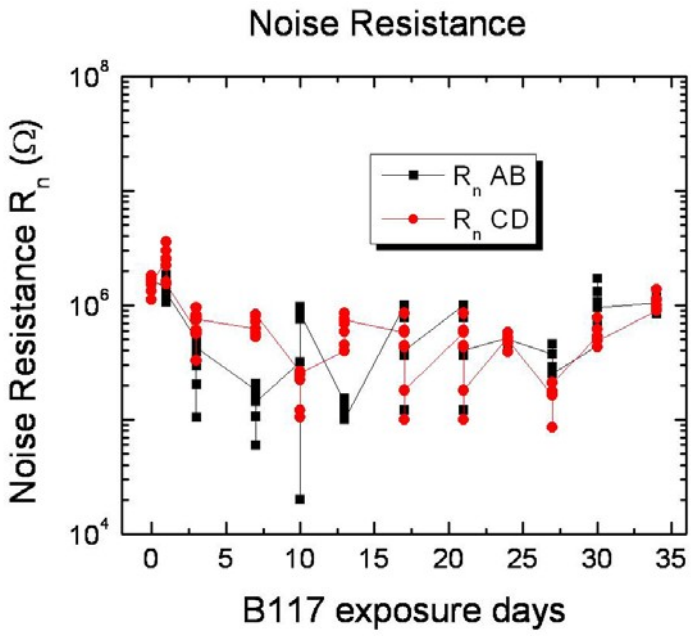

Figure 11. Noise resistance Rn between sensor AB and CD.

The experimental results above have shown that the sensors were successfully embedded between the Mg- rich primer and topcoat system. Further, they did pick up the coating's electrochemical property changes during the B117 salt fog exposure. The 2E sensor EIS showed similar results as the conventional 3E EIS testing, which confirms the feasibility of *in situ* monitoring of coatings' electrochemical properties by embedded sensors. The electrochemical noise measurement could also pick up the signal from the coating property changes, but proved to not be as sensitive as EIS in localizing the signal with respect to the experimental area.

For more details on the above experiments, refer to Appendix A "Embedded sensor electrode arrays for real time monitoring of an Air Force topcoat/Mg-rich primer systems." This paper has been accepted for publication in the journal *Corrosion Science*.

2.3 In Situ Monitoring of a Mg-Rich Primer Under a Topcoat Under Prohesion® Conditions

Mg-rich primers have been proven to be an adequate alternative for chromate-based coatings [Nanna, 2004] for the protection of aluminum alloys from corrosion. Its protection behavior was attributed to a combination of cathodic and barrier protection [Battocchi 2006 (1 and 2)], similar to the protection behavior associate with Zn-rich primers on steel substrates.

The performance of a Mg-rich primer on aluminum 2024-T3 under Prohesion® exposure (ASTM G85) has been monitored using an embedded sensor placed at the surface of the primer and below the topcoat. This accelerated weathering cycle is an alternative of wet and dry cycles to simulate outdoor weather exposure. Prohesion® exposure is a less severe version of the standard salt spray tests and is generally regarded as giving a better correlation with outdoor exposure results. The method involves mounting the test panels in a chamber into which is introduced an aqueous solution of salts in the form of a fine aerosol. The method differs from the standard salt spray tests in that the salt solution used in the Prohesion® exposure test is much more dilute and the panels are not exposed to it continuously.

Electrochemical impedance spectroscopy and electrochemical noise methods experiments were conducted to monitor the performances and the electrochemical properties of the system beneath the topcoat. The data analysis demonstrates that the sensor is able to detect changes in the barrier property of the topcoat in response to the exposure conditions and the activation of the active pigments in the primer in presence of the electrolyte.

The Mg-rich primer and polyurethane clear topcoat system were applied onto the AA2024-T3 substrate, and the platinum sensor was embedded between the primer and the topcoat. Afterwards, the coated substrate was put into the standardized Prohesion® chamber to simulate weathering conditions in an aggressive manner to induce accelerated coating failure. The acquisition of EIS and ENM data from embedded sensor in-situ monitoring during the Prohesion® dry and wet steps demonstrated the coating behavior evolution. In this study, it was found that both EIS and ENM in-situ monitoring could be conducted under either dry or wet Prohesion® steps with the embedded sensors. Under the dry step, the coatings were sensitive to temperature changing, while in the wet step, the resistance values were more scattered due to the moisture accumulation on the coating surface. Both the temperature and humidity variation related coating property changes in Prohesion® chamber were *in situ* monitored by the embedded sensors. It was found that the coating degraded continuously with Prohesion® exposure time shown by a continuous decrease both in low frequency impedance $|Z|_{0.05\ Hz}$ and noise resistance R_n.

For detailed description of this experiment, refer to Appendix B, “In Situ Monitoring of a Mg-Rich Primer Beneath a Topcoat Exposed to Prohesion® Conditions.” This paper was presented at the NACE Conference in San Antonio, TX in January 2010 and has been accepted for publication in the journal *Corrosion Science*.

2.4 Remote Corrosion Sensor Design

The wireless sensor array has the potential to be deployed widely for coating evaluation. The embedded sensor electrodes developed at NDSU and described above (Section 2.1) is designed to work with a variety of miniaturized electrochemical interfaces (potentiostats) equipped with a wireless interface. Such approach enables ***remote*** health monitoring of structural parts, remote areas, and hard-to-reach and enclosed spaces (e.g. fuel tanks).

The PG581 potentiostat – galvanostat from Uniscan Instruments featured in Figure 12 is a compact and powerful hand-held device for electrochemistry and corrosion applications. The instrument is designed to perform both in the laboratory and as a user configurable instrument in the field. The PG581 is ideally suited for the in-field development of electrochemical sensor technologies, and as a cost-effective portable electrochemical and corrosion analyzer.

The PG581 potentiostat - galvanostat is connected to a PC via its USB port in the laboratory for electrochemical experiments with unsurpassed ultralow noise performance. In addition, the operator can upload those same techniques directly to the PG581 to collect data in the field without the use of a PC.The PG581 also provides support for the routine electrochemical corrosion techniques such linear polarization, Tafel, potentiodynamic polarization and many other. The PG581 plots experimental data in real time on graphics screen and/or saves the data on a removable miniSD card. In addition to the features above, the PG581 is capable of operating on internal rechargeable battery power, which makes it indispensable in applications with frequent power failures or where stable supply of power is impossible due to logistic of physical factors.

Figure 12. Uniscan PG581 potentiostat-galvanostat.

Unlike any other device on the market, the PG581 is capable of running electrochemical test on up to five channels in sequence without the use of an external multiplexer. This feature of the PG581 is crucial to the successful implementation of health monitoring system based on an array of corrosion sensors. The five-working electrode cable shown in Figure 13 has 8 leads – 5 for working electrodes (5 sensors), one is connected to a reference electrode, one to a counter electrode, and there is also a ground lead.

Figure 13. Five-electrode multiplexed cable for PG581.

The software package allows the user to easily set up the experiment protocol to address up to five working electrodes using the multiplexed cable shown in Figure 13. Normally, an external multiplexer would be required to carry out electrochemical test on more than one electrochemical cell. A multiplexer is an electronic switch which under computer control automatically moves the control and acquisition circuits of the single channel potentiostat from one working electrode to another. The PG581 has a built-in multiplexer. Having an on-board multiplexer and potentiostat in one compact device allows NDSU to proceed to the next stage of wireless sensor development – wireless node integration.

Figure 14 shows a diagram of the wireless node implementation using corrosion sensors described in Section 2.1. The location of embedded sensors electrodes on the Boeing C-17 is merely chosen to illustrate the concept and does not represent the true placement of sensors on an aircraft in the field. The PG581 is capable of driving up to five sensors installed on an aircraft structure. It then acts as both electrochemical interface (potentiostat) and multiplexer. The available USB connector on the PG581 is then connected to a wireless USB hub, which in turn communicates with a host computer, from which an operator can control and programs the potentiostat, upload experimental scripts to the potentiostat and download raw data for subsequent data analysis and storage.

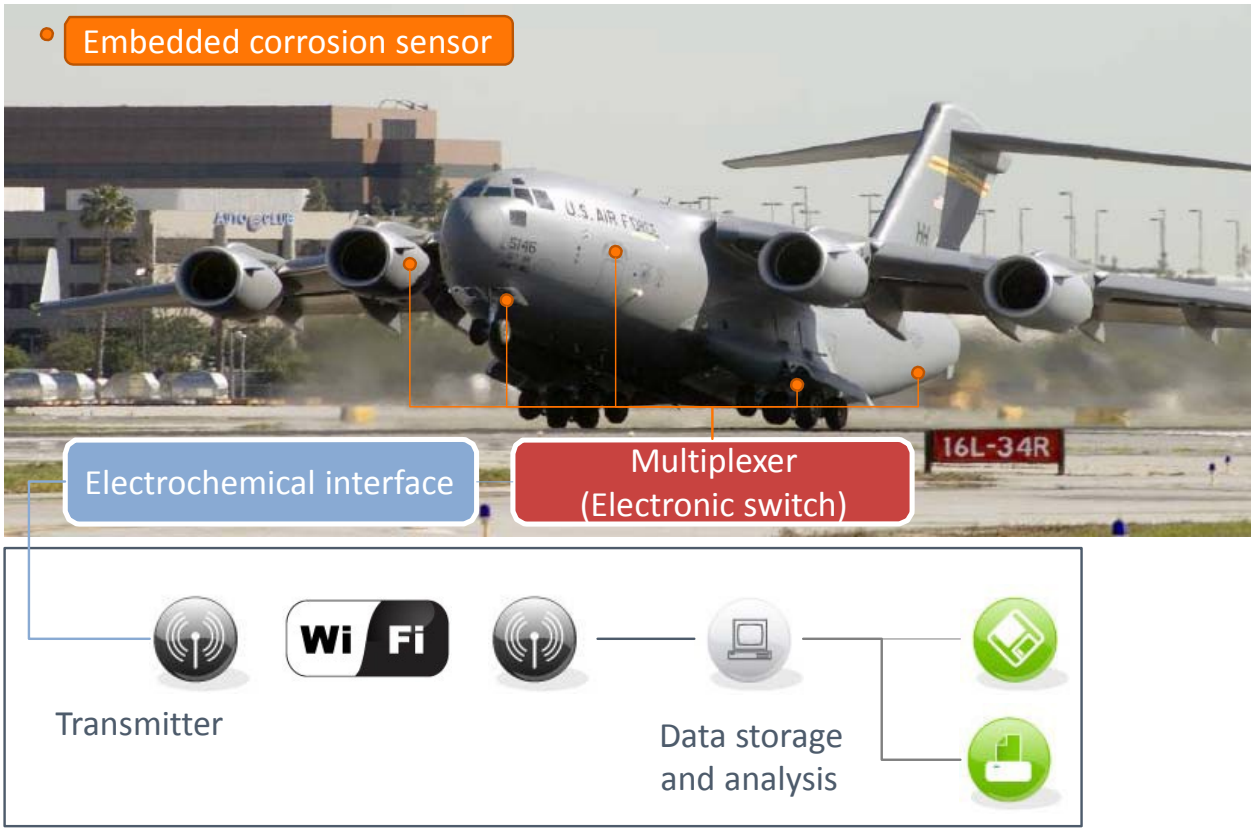

Figure 14. Corrosion sensor node with wireless communication.

In terms of wireless communications, there are a variety of choices currently available on the market. The IEEE 802.11 standard, often called Wi-Fi, approaches speeds of some types of wired Ethernet. However, such devices have demanding power requirements. An IEEE 802.15.4 protocol, less known to consumers is a specification for a suite of high level communication protocols using small, low-power digital radios. The technology, defined by the ZigBee specification, is intended to be simpler and less expensive than Wi-Fi and Bluetooth. ZigBee is targeted at radio-frequency (RF) applications that require a low data rate, long battery life, and secure networking. In the case of wireless health monitoring, high data rate is not crucial, as the PG581 is able to store data internally without having an always "on" communication channel with the host device.

ZigBee is a low-cost, low-power, wireless mesh networking standard. First, the low cost allows the technology to be widely deployed in wireless control and monitoring applications. Second, the low power-usage allows longer life with smaller batteries. Third, the mesh networking provides high reliability and more extensive range. ZigBee operates in the industrial, scientific and medical (ISM) radio

bands; 915 MHz in the USA and Australia, 868 MHz in Europe, and 2.4 GHz in most jurisdictions worldwide.

Because ZigBee can activate (go from sleep to active mode) in 30 msec or less, the latency is very low and devices are very responsive — particularly compared to Bluetooth wake-up delays, which are typically around three seconds. Because ZigBees can sleep most of the time, average power consumption can be very low, resulting in long battery life.

Figure 15 demonstrates the concept of integration of the corrosion sensors described in Section 2.1 into a real-life structural aircraft part in one possible application of a corrosion sensor near a rivet. The underside of a riveted part of an aircraft structures is shown in this figure. The sensor is located on the other side of the panel near the rivets, at a distance dictated by the specific application of the sensor. The conductive interconnect follows the surface to a rivet, then it penetrates the structure to the side that is visible in Figure 15 (from bottom to top of the panel), where an electrical connection to the potentiostat is made. The interconnect passes the rivet through a small insulated hole. The insulation is necessary to avoid short-circuiting the sensors and current leakage through the structure.

Figure 15. Mock-up sensor arrangement on structural aircraft part showing possible sensor connection to potentiostat and multiplexer.

The sensor electrode interconnect was protected by an adhesive film with an opening of a fixed size, as shown in Figure 16.

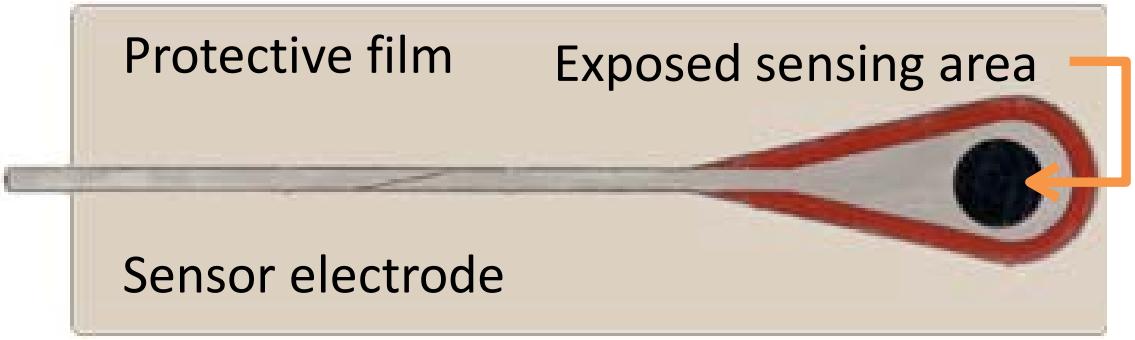

Figure 16. Embedded sensor electrode with an applied film mask.

The permanent adhesive film was obtained from Avery (Brea, CA). Such film is often used in RFID design for flexible antenna manufacturing. However, it was not known whether the film would protect the sensor in corrosive electrolyte. An EIS experiment was carried out, where both bare AA2024-T3 substrate and the same substrate with an applied film were immersed in dilute Harrison's solution, as shown in Figure 17. EIS tests were carried out in 3-electrode cell at 10 mV ac applied ac potential in the frequency range from 100 kHz to 10 mHz.

Within 2 hours of immersion on day 1, the bare substrate shows low-frequency impedance modulus, |Z|, values on the order of 5 x 10^3 Ω, which is expected of unprotected Al alloy. Upon further immersion, the |Z| value did not change appreciably.

For the substrate with the applied film, the |Z| value fluctuated significantly after 2 hours of immersion in DHS, between 10^{10} and 10^{13} Ω, which is indicative of very high impedance that the instrument is incapable of measuring reliably. As the cell was allowed ample time to equilibrate after 1 week of constant immersion in DHS, the low-frequency |Z| stabilized around 10^{10} Ω, being almost 7 orders of magnitude higher than |Z| for bare Al. Values about 10^9Ω indicate a highly protective film; therefore, the Avery 5663 adhesive mask affords adequate protection against electrolyte and will be used for masking off the sensing area of an embedded corrosion sensor for remote health monitoring.

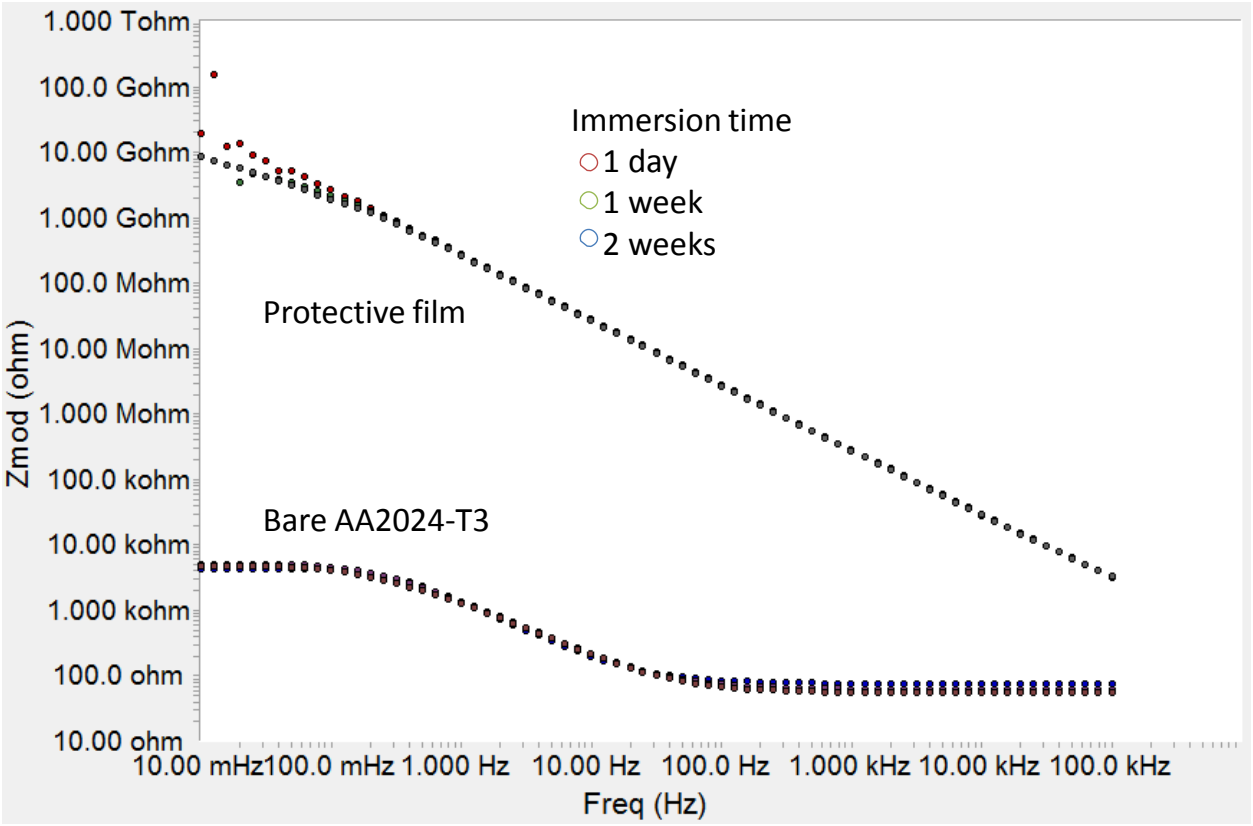

Figure 17. EIS response of AA2024-T3 with and without insulating film.

3.0 Summary and Conclusions

A new flexible circuit corrosion sensor electrode was designed that was shown to be robust, reproducible, thin, flexible, and adaptable to various field applications. The shape and size of the sensor could be easily changed by creating the appropriate shadow mask for metal deposition. The sensors are not limited to the use of platinum or other expensive metals.

The Mg-rich primer and polyurethane clear topcoat system was applied onto AA2024-T3 substrates, and platinum sensors were embedded between the primer and the topcoat. Then the coated substrates were put into the standardized Prohesion® chamber to simulate weathering conditions in an aggressive manner to induce accelerated coating failure. The acquisition of electrochemical impedance spectra and electrochemical noise measurements data from embedded sensor in-situ monitoring during the Prohesion® dry and wet steps provided insight into the coating behavior evolution. It was found that both EIS and ENM in-situ monitoring could be conducted with embedded sensors under both dry and wet Prohesion® steps. Under the dry Prohesion® step, the coatings were sensitive to the temperature changes, while in the wet step, the resistance values were more scattered due to the moisture accumulation on the coating surface. The effects of both the temperature and humidity variation on changes in coating properties were in-situ monitored by the embedded sensors in Prohesion® chamber. It was found that the coating degraded continuously with Prohesion® exposure time as evidenced by the gradual decrease of both low frequency impedance $|Z|_{0.05\ Hz}$ and noise resistance R_n. Further, the 2-electode Sensor-Sensor electrochemical impedance data agreed well with the data obtained from the conventional 3-electrode setup performed in a laboratory environment, thus demonstrating the feasibility of this 2 sensor electrode approach without the need of additional reference or counter electrodes.

4.0 References

D. Battocchi, J. He, G.P. Bierwagen, and D.E. Tallman, *Emulation and study of the corrosion behavior of Al alloy 2024-T3 using a wire beam electrode (WBE) in conjunction with scanning vibrating electrode technique (SVET),*Corrosion Science, **2005**, 47(5), 1165-1176.

D. Battocchi, A. M. Simoes, D. E. Tallman and G. P. Bierwagen, Corr. Sci. **2006**a, 48, 1292.

D. Battocchi, A. M. Simoes, D. E. Tallman and G. P. Bierwagen, Corr. Sci. **2006**b, 48, 2226.

G.P. Bierwagen, M.E. Nanna, D. Battochi. *Magnesium-rich coatings and coatings systems*, 2004-US33089, 2005051551, 20041007, **2005**.

M. E. Nanna and G. P. Bierwagen, J. Coating technol. Res. 2004, 1, 69.

C. L. Wu, X. J. Zhou, Y. J. Tan; *Progress in Organic Coatings*, **1995**, 25, 379-389.

5.0 Program Management

The Durable Hybrid Coatings program has the following management structure:

- Technical Manager for Department of Coatings and Polymeric Materials activities: Dante Battocchi, Research Assistant Professor, Department of Coatings and Polymeric Materials.
- Senior Scientific Advisor: Dr. Gordon Bierwagen, Professor, Department of Coatings and Polymeric Materials. [PI of record]
- Dr. Vsevolod "Séva" Balbyshev, Research Scientist, Center for Nanoscale Science and Engineering, coordinates new work on aircraft health prognostics.
- Program Manager and management POC for AFRL: Dr. Larry R. Pederson, Director, Center for Nanoscale Science and Engineering. Dr. Gregory J. McCarthy formerly served in this capacity until his retirement as Director of CNSE.

One Post-Doctoral Research Associate and one Graduate Research Assistant worked on this project during the past year. They are:

- Dr. Duhua Wang, Department of Coatings and Polymeric Materials, and
- Mr. Hong Xu, Department of Coatings and Polymeric Materials.

The Durable Hybrid Coatings program at AFRL was initiated in July 2004, and with the supplement for new work added in 2008, the end date is now May 2011. An Annual Progress Report is prepared each year, with a Final Report due after the close of the program.

6.0 List of Acronyms

ASTM – American Society for Testing and Materials (http://www.astm.org/)

CNSE – Center for Nanoscale Science and Engineering (http://www.ndsu.edu/cnse/)

CPM – Coatings and Polymeric Materials (http://www.ndsu.edu/cpm/)

EIS – Electrochemical impedance spectroscopy

2-E EIS – 2-Electrode electrochemical impedance spectroscopy

3-E EIS – 3-Electrode electrochemical impedance spectroscopy

MRP – Magnesium-rich primer

NACE – National Association of Corrosion Engineers (http://www.nace.org)

NDSU – North Dakota State University (http://www.ndsu.edu)

OCP – Open circuit potential, E_{oc}

R_n – Noise resistance

SCE – Saturated calomel electrode

|Z| - Impedance modulus

$|Z|_{0.05\ Hz}$ – Low-frequency impedance modulus at 0.05 Hz

7.0 Financial Summary

The following table summarizes expenditures on the program through September 20010.

Durable Hybrid Coatings
Cooperative Agreement FA8650-04-1-5045
Annual Report for Period ending September 30, 2010

	July-04 through Sept-09	Oct-08 through Sept-10	Total Expenditures	Budget	Balance
Personnel	$1,903,267	$331'141	**$2,234,408**	$2,331,828	$97,420
Direct Operating Costs	$617,965	$36,901	**$654,867**	$684,923	$30,056
Subcontracts	$154,008	$0	**$154,007**	$154,007	$0
Capital Equipment	$470,447	$24,269	**$494,716**	$494,716	$0
Indirect (F&A) Costs	$1,079,667	$168,571	**$1,248,238**	$1,304,326	$56,087
Total	**$4,225,354**	**$560,883**	**$4,786,237**	$4,969,800	**$183,563**

APPENDIX A

Corrosion Science 2011 (in press)

EMBEDDED SENSOR ELECTRODE ARRAYS FOR REAL TIME MONITORING OF AN AIR FORCE TOPCOAT/MG-RICH PRIMER SYSTEM

V.N. Balbyshev, K.N. Allahar,* D. Battocchi,* G. Strommen, and A. Reinholz
Center for Nanoscale Science & Engineering,
NDSU Dept 4310, Fargo, ND 58108
Department of Coatings and Polymeric Materials
North Dakota State University
NDSU Dept 2760, Fargo, ND, 58108 seva.balbyshev@ndsu.edu,
kerry.allahar@ndsu.edu, dante.battocchi@ndsu.edu, greg.strommen@ndsu.edu,
aaron.reinholz@ndsu.edu

ABSTRACT

Mg-rich primers are chromate-free alternatives that are currently used by the Air Force for the protection of aluminum structures. Magnesium pigments undergo anodic dissolution thus protecting the less electrochemically active aluminum substrates. At the same time, corrosion products of Mg dissolution act as a barrier that insulates the substrate from corrosive environment. Characterization of a standard Mg-rich primer/Air Force urethane topcoat was carried out by electrochemical impedance spectroscopy (EIS) and on coated AA2024-T3 substrates subjected to exposure conditions according to a constant immersion test protocol. Sensor electrodes of a newly-developed design were made by the industry standard selective laser etching procedure utilized by many common printed circuit board manufacturers. Unlike conventional electrochemical sensors that monitor the metal substrate itself and provide no information about the coating, these corrosion sensors are embedded between the primer and the topcoat and thus are suitable for monitoring the corrosion protection afforded by the metal-rich primer. As an added advantage, the embedded sensor electrodes are shielded from the environment by the topcoat. This prolongs the electrode life, as well as reduces the noise associated with measurement. The sensor electrodes of different surface areas were embedded between the primer and the topcoat. An array of sensor electrodes was used to assess the behavior of the Mg primer underneath the topcoat. Experimental results demonstrated the feasibility of the embedded sensor electrode array approach to monitor cathodic protection of Mg-rich primers on structural aluminum alloys by in situ and electrochemical impedance spectroscopy (EIS) technique. The presented embedded sensor electrode array is part of the effort aimed at development of wireless corrosion sensors for monitoring cathodic protection of metal-rich primers.
Keywords: Mg-rich primer, embedded sensors, EIS

INTRODUCTION

Aluminum alloys, especially AA2024-T3, are widely used in the aerospace industry because of their high strength and stiffness combined with low density. However, Al alloys are very sensitive to corrosion environments due to their high copper content. Currently, chromate pre-treatment and chromate primer coatings are used to protect aluminum alloys from corrosive attacks.[i] Current coating systems for aircraft corrosion protection are based on a traditional chromate surface treatment, primer, and topcoat. To date, the corrosion protection of aluminum alloys has relied extensively on potent hexavalent-chromium compounds, which are included in both surface preparation/treatments and organic primers. However, the toxicity and carcinogenic properties of chromium has caused federal agencies, in particular the EPA, to impose severe restrictions on its use.[ii] Corrosion protection of aluminum-skinned aircraft and development of improved environmentally benign surface treatments for aluminum aerospace alloys are critical needs for the aerospace industry. Recently developed metal-rich coatings for corrosion protection of aircraft aluminum alloys rely on magnesium powder dispersed in an organic binder. It has been shown that this environmentally friendly formulation of Mg-rich coatings can provide exceptional protection for aluminum-based alloys.[iii,iv] In these metal-rich coatings, Mg particles embedded in a polymeric matrix act as a sacrificial anode; Mg undergoes anodic dissolution and thus protects the underlying metal from corrosion. By analogy to the Zinc-rich primer coatings that keep steel from corrosion through cathodic protection, the Mg-rich primer (MRP) coatings, were designed, examined and developed by M. E. Nanna, D. Battocchi and G. P. Bierwagen at NDSU.[v,vi] By using pure magnesium pigment, which is more active than aluminum alloy substrate, Mg-rich primers were formulated around the Critical Pigment Volume Concentration (CPVC) to make sure there are good electrical conductivities among pigment particles and between pigment and substrate. This work motivated by the need for chromate-free alternatives for protection of high-strength aircraft Al alloys such as AA2024-T3 and AA7075-T6. G.P. Bierwagen and the corrosion group at NDSU are leading this Mg-rich primers research and a series of articles have been published on their application and properties.[vii, viii]

Recently, there has been extensive development of several in situ sensing techniques that monitor the barrier properties of a coating. Most research in electrochemical sensors has been focused on sensor electrodes embedded in the substrate. Such sensors monitor corrosion of the metal substrate but provide no information about the film itself. Thus, they are unsuitable for monitoring corrosion within the metal-rich primer itself.

A new technique for in situ monitoring of a coating with ac involves the application of an embedded electrode or sensor within the coating. There are only a limited number of groups globally that are actively involved with the application of the embedded sensor technology.[ix - xi] The Department of Coatings and Polymeric Materials and Center for Nanoscale Science and Engineering at NDSU have been at the forefront in the development, feasibility demonstration, and application of embedded sensors, which consist of electrodes that act as the counter and reference but are placed between the layers of two-layered coating systems.[xii, xiii] A schematic diagram of the embedded sensor is shown in Figure 1. An advantage of the embedded electrodes is that they are shielded from the environment by the topcoat, which prolongs the electrode life as well as reduces the noise associated with measurements. Another advantage is that electrochemical measurement of the primer and primer/metal interface can be made without being masked by high resistant topcoats.

Until now, the embedded sensors approach has been applied for characterization of standard Air Force and Army vehicle coatings that are evaluated by thermal cycling accelerated testing method,[xiv] and accelerated ac-dc-ac testing method.[xv] While there have been limited studies published on the use of embedded sensors in the aforementioned coating systems, there has been no application to metal rich primers, e.g. Mg- or Zn-rich primers. The coupling of embedded sensors and coating systems with Mg-rich primers is a unique approach that allows in situ monitoring of the electrochemical behavior of protective Mg-rich primers beneath a topcoat.

The newly-developed embedded sensor electrode array is part of the effort aimed at development of wireless corrosion sensors for monitoring cathodic protection of metal-rich primers. Sensor electrodes of a new design were made by the industry standard selective laser etching procedure utilized by many common printed circuit board manufacturers. Sensor electrodes of different surface areas were embedded between the primer and the topcoat. An array of sensor electrodes was used to assess the behavior of the Mg primer underneath the topcoat. Sensor arrays were manufactured in a multi-stage process, involving standard industrial deposition procedures using industrial grade equipment.
Electrochemical Impedance Spectroscopy (EIS) is a fast and useful method widely applied in monitoring and evaluating the performance of organic coatings, especially the corrosion protection abilities. In this study, EIS was used to characterize the electrochemical performances of Mg pigmented primers as a function of exposure time.

EXPERIMENTAL

The protective coating system used in the experimental procedure was composed of a high solids polyurethane gloss enamel (AKZO NOBEL 646-58-7925 with AKZO NOBEL X-501 curing component) and a Mg-rich primer developed at NDSU.[xvi] In this primer, Mg powder with the average particle size of 25 μm (Ecka Granules of America, Orangeburg, SC) was dispersed in a two-component epoxy-polyamide resin, and the pigment volume concentration (PVC) of the primer was 45%. The primer was applied to standard panels of aluminum alloy AA2024-T3. After the application of the primer, the sensor was applied on the surface of the primer, followed by the application of the polyurethane topcoat.

Sample preparation

The aluminum alloy 2024-T3 panels, 4" x 8" in size were polished by 200 grit followed by 600 grit sanding paper, then washed with hexane and dried with a nitrogen flow. The freshly pretreated metal panels were coated within half an hour after they were polished.
Four platinum circuit sensors on Kapton® backing, manufactured at NDSE Center for Nanoscale Science and Engineering (CNSE), were placed on cleaned 4" x 8" aluminum panels.
A thin layer of a homemade epoxy resin (D.E.R. 331 epoxy resin/Ancamide 2353/methyl ethyl ketone at a 5/3/5 weight ratio) was applied to the Pt track connecting the sensor pad to the wire terminals. The arrangement of the sensors on the test panel is shown in Figure 2. After 10 minutes of solvent flash-off, a few drops of the epoxy were placed on the primer, and the circuit sensors were then adhered onto the primer. The primer and the glued sensors were given one day to harden at room temperature before the polyurethane topcoat was applied. The approximate neat dry film thickness of Mg-rich primer was 40±5 μm, and 80±10 μm for the topcoat.

Experimental Configurations

The in situ monitoring of the Mg-rich primer and polyurethane topcoat paint system was carried out under constant immersion conditions. Electrochemical Impedance Spectroscopy (EIS) was collected on a Gamry PCI4-300 potentiostat coupled with Corrosion Measurement System CMS100 and CMS300 software. Detailed description of this electrochemical technique can be found elsewhere.[xvii], [xviii] The spectra were obtained in the frequency range from 10 mHz to 100 kHz at 10 mV RMS imposed ac potential (vs. Eoc).
Both the two-electrode (2E) cell for sensor-to-sensor measurements and three-electrode (3E) cell arrangement for sensor-to-substrate measurements were used to obtain the EIS responses in a one-panel setup, where a coated panel was assembled with four sensors placed in rows of two as shown in Figure 3 (a). Areas marked with circles are exposure areas subjected to constant immersion in dilute Harrison's solution (DHS) (0.05 wt% NaCl / 0.35% (NH4)2SO4, pH=5.5). The scribed and un-scribed areas were exposed to DHS by virtue of clamping a glass cell with an o-ring over the corresponding spot, resulting in a total exposure area of 6.45 cm2. For the sake of simplicity, the individual sensors in positions 1, 2, 3, and 4 in Figure 3 (b).will be referred to as Sensor 1, Sensor 2, etc. For the 3-electrode setup, a platinum mesh counter electrode and saturated calomel reference electrode (SCE) were utilized in a three-electrode

configuration. In the 2-electrode arrangement, one sensor was connected to the working electrode and the other sensor connected to the counter and reference electrodes.

Results and Discussion

Flexible Circuit Sensor Design

The feasibility of Pt-mesh embedded sensors developed at NDSU for monitoring the effectiveness of Mg-rich primers has been documented previously.12-14 In these studies, embedded sensors were either completely immersed in corrosive electrolyte or were subjected to cyclic salt fog environment, and thus the area surrounding the sensors was corroding at approximately the same rate as the entire panel. In this case, for the sensor to accurately detect corrosion, it is important to design a sensor in such a way as to not to impede the ingress of electrolyte and allow it to reach the Mg-rich primer and trigger corrosion reactions in the system. She U-shape design of these sensors suited extremely well for this purpose. However, one of the drawbacks of Pt-mesh sensors is their delicate nature. At thicknesses of 120 nm, Pt-mesh sensor had to be handled with care, application of sensors required specially trained lab personnel. Additionally, the wires protruding from the test sample made it ideal for laboratory use, but made them impractical in the field.

Researches and engineers and NDSU CNSE have used the available technologies for circuit printing in designing a new prototype of the sensor that would address the two main drawbacks of the Pt-mesh sensor. In addition to being robust and reproducible, the new sensor would be flexible as to allow easy application to a range of geometries of structural parts.

The new "circuit sensor" was made to resemble the U-shape design of the Pt-mesh sensor in order for researchers to do similar type of experimentation with embedded sensors in application involving metal-rich primers. Instead of making a sensor into a simple (rectangular or circular) planar shape, a provision for ingress of electrolyte was made in the form of conducting 'fingers' separated by gaps of varying widths allowing for electrolyte to penetrate into the primer. Initially, the widths of the fingers and spacings between them ranged from 250 μm to 2000 μm, resulting in nine different finger/spacing configurations. Sensor design is shown in Figure 4 displays two sensors with different finger-spacing dimensions. The sensor design concept shown in Figure 4 was translated into a CAD drawing using Design Capture/Expedition by Mentor Graphics (Mentor Graphics, Wilsonville, OR). Sensor design took into consideration the embedded aspect of the corrosion sensor.

In the next step, the inverted image of the sensor generated by CAD software was used to manufacture a shadow mask (stencil) for subsequent physical vapor deposition of metallic film (conductive path of a sensor). The stencils were made from series 316 stainless steel by Great Lakes Engineering (Maple Grove, MN). Initially, nine variations of stencils with varying finger and spacing widths were manufactured. The deposition step was performed at NDSU CNSE on a CMS-18 PVD sputtering sustem (Kurt J. Lesker Company, Clairton, PA). For better adhesion, a 50 Å layer of Cr (99.95% pure, from Kurt J. Lesker Company, Clairton, PA) was first vapor deposited on a 2 mil thick Kapton® film (obtained from McMaster-Carr, Robbinsville, NJ), followed by the deposition of 1500 Å layer of Pt (99.99% from Equipment Support Company USA Inc., Pensacola, FL).

Following the deposition, the Kapton® pieces, 15 cm in diameter each, were transferred to the Optec MicroMaster laser ablation station (Z.A.E. Le Crachet, Frameries, Belgium) where the spacings between the fingers were cut out by laser. During the laser ablation step, it was discovered that sensors with closely spaced narrow fingers were difficult to ablate, and frequent laser cutting generated too much debris. In order to streamline the manufacturing process and reduce the duration of the laser ablation step, two sensor electrode geometries were selected for testing: 1 mm thick fingers spaced at 0.5 mm and 1 mm, as shown in Figure 4.

After the ablation step, excess Kapton® around the conductors was removed, and the sensors were cleaned by ionized oxygen in March Plasma Treatment System (March Plasma Systems, Concord, CA), rubbed in IPA, and immersed in an ultrasonic bath. The resulting sensors are shown in Figure 5. Each sensor is composed of a pair of individual sensor electrodes. A metal substrate, 4" x 8" in size, accommodates four individual sensor electrodes of one particular design. The electrical connection to

sensor electrodes was made by clipping an instrument lead to a metal screw (post) connected to the terminal pad shown in Figure 2. Two pairs of sensor electrodes (4 sensor electrodes per panel) with different spacings between conductive fingers are shown in Figure 6. The width of the fingers for both Wide and Narrow sensors is 1 mm. The fingers are spaced apart by 500 μm for the Narrow sensor, and 1000 μm for the Wide. The sensing area of each sensor electrodes is 16 x 16 mm2. After the application of the top-coat, two areas of interested (marked by circles in Figure 3) were identified on the surface of the coated specimen. The area between Sensor electrodes 1 and 3 was scribed using Gravostar engraving machine (Gravostar USA, Chillicothe, OH). This exposure area will be referred to as Scribed, while the area between Sensors 2 and 4 remained intact and will be referred to as Non-scribed. Such experimental setup differs from the earlier approach that subjects the entire panel to electrolyte attack. Incorporation of glass cylinders to carry out constant immersion exposure ensures that any degradation experienced by the sensors will come from a defect area through the coating along the plane of the substrate (longitudinal diffusion) vs. ingress of electrolyte through the top-coat directly above the sensor. The former arrangement reflects field conditions more accurately.

Electrochemical Tests

In order to investigate the feasibility of the new flexible circuit sensor electrodes, series of electrochemical tests were performed on the embedded sensors both in 2-electrode and 3-electrode cell configurations. For simplicity, the individual sensors in positions 1, 2, 3, and 4 in Figure 3 (b) will be referred to as Sensor 1, Sensor 2, etc. During off-test time, both glass cells were filled with DHS. During electrochemical tests, the solution was drained from the cell that was not being investigated. The cells were allowed at least an hour for the open circuit potential to reach steady state for the cell under test, and for the solution to dry out in the case of the other cell. The 3-electrode setup was utilized to measure the response of individual sensor, while the 2-electrode approach was used to make sensor-to-sensor measurements, as described in the Experimental section. During EIS tests, it as noted that the difference in electrochemical responses from the sensor electrodes with wide and narrow spacings were within 5-7%. Given the much greater fluctuation of impedance response as function of time, only one value for each electrochemical parameter is reported. For the purposes of this discussion, both Narrow and Wide sensors will be referred to as Sensor, followed by the numeric designation based on the sensor position on the test panel.

The open circuit potential was measured before each EIS test to ascertain that the system had had adequate time to equilibrate before the measurement. In addition, open circuit potential is a very important parameter for monitoring corrosion of metal-rich primers, as it provides information about the electrochemical state of the system.

For the non-scribed panels, the decrease of Eoc with time is indicative of gradual progression of corrosion, as seen in Figure 7. For the specimens without a top-coat, the Eoc would typically reach the corrosion potential of Mg alloy over time. However, for top-coated panels, the Eoc is typically several hundred millivolt higher. The overall Eoc of the entire panel, labeled as Panel on the graph in Figure 7, decreases with immersion time. However, Sensor 4, which is located near the non-scribed area, while exhibits the same trend as Eoc for Panel, shows Eoc values 200-300 mV higher than for Panel. This is explained by the fact that Eoc is measured over non-exposed area across dry Mg-rich primer. The distance between the SCE reference electrode and Sensor 4 is about 2 inches, whereas Eoc for Panel is measured between the reference electrode in the non-exposed sell through the 40-μm layer of MRP.

In the 2-electrode setup (sensor-to-sensor, S1-S4 and S3-S4), a different trend is observed for Eoc as a function of immersion time. The Eoc decreases at first, followed by a gradual increase after one month of immersion. While the absolute values of Eoc are meaningless in this instance, as there is no actual reference electrode employed in this setup, the trend shown in Figure 7 can be explained by at least one electrode (Sensor 1) being in the vicinity of a scribed area which had suffered from corrosion. Therefore, the Eoc decrease and subsequent increase follow the expected Eoc behavior of MRP systems. The increase in Eoc is related to the accumulation of corrosion products in the area adjacent to Sensor 1. It is

also possible that Sensor 1 is 'shorting' through the substrate, in which case it is electrically connected to the scribe site.

For the un-scribed system, the Eoc for Panel and sensor-to-sensor 2E pairs show a trend towards more positive values as immersion progresses, as seen in Figure 8. This behavior is characteristic of active metal corrosion and protective action of MRP. The initially low values of Eoc indicate that by the time the first measurement is made on the system, it is already corroding. Upon further exposure to DHS, the corrosion products formed by the dissolving Mg pigment result in a formation of a passive layer that gives rise to impedance modulus and Eoc. For Sensor 4, however, the observed Eoc trend is reverse and parallels that of the un-scribed specimen. This could be explained that Sensor 4 is not electrically connected to the site of the scribe, and thus its Eoc response is unaffected by this defect. For Sensor 5, Eoc trends for scribed and un-scribed areas are remarkably similar.

Figures 9 and 10 show the low-frequency impedance moduli measured at 10 mHz frequency. The low-frequency impedance modulus |Z10 mHz| for the non-scribed site is displayed in Figure 9. For brevity, the notation |Z10 mHz| will be replaced by |Z| from this point on. For the entire panel, the |Z| measured in a 3-electrode setup decreased with time. This observation is consistent with the shift in Eoc towards more negative values. The entire panel is gradually losing its barrier properties, thus |Z| decreases from 2 x 109 Ω cm2 to 5 x 108 Ω cm2, an order of magnitude over the period of 2 months of constant immersion. For the 2-electrode arrangements, EIS response of individual sensors (3 and 4) follow the trend for the entire Panel. However, |Z| values for Sensor 4 are almost an order of magnitude higher than those for Sensor 3. This is the result of the Sensor 4 being more distant from the defect on the panel.

In the case of the scribed area, |Z| for the entire panel and Sensor 3 increases slightly over the 2 months immersion period (Figure 10). This observation is consistent with the Eoc trend. The formation of a passive layer of corrosion products results in a slight increase in the low-frequency modulus. Sensor 3 is close to the scribe area, and therefore its response is expected to parallel that of the overall panel when measured at the scribe.

|Z| values for Sensor-to-Sensor arrangements (S1-S4 and S3-S4) and Sensor 4 remain virtually unchanged with time, yet slight increase is observed after a 3-week mark. The observed trend is due to Sensor 4 not being affected by the corrosion processes taking place at the scribe. The values for sensor-to-sensor configurations and Sensor 4 are 3 orders of magnitude higher than those for the entire Panel and Sensor 3, which is explained by Sensor 4 not being in electrical contact with the corroding area at the scribe.

Based on the above results, it can be said that flexible circuit sensor is suitable for monitoring corrosion protective activity of Mg-rich primers. The electrochemical response detected through this sensor is influenced to the great degree by the area immediately surrounding the sensor when used in a 2-electrode, sensor-to-sensor configuration. However, this is viewed as rather the limitation of the electrochemical impedance technique than the sensor itself.

CONCLUSIONS

A new flexible circuit sensor electrode was designed at NDSU Center for Nanoscale Science and Engineering. Such electrode is robust and reproducible, while at the same being thin, flexible, and adaptable to various field applications. The shape and size of the sensor can be easily changed by creating the appropriate shadow mask for metal deposition. The sensors are not limited to the use of platinum or other expensive metals. However, selection of materials for the conductive aspect of the sensor must conform to the requirements of a particular application. The use of platinum in this design was dictated by its superior conductivity at nanometer thicknesses and by the available of experimental electrochemical data for embedded sensors for Mg-rich primers. The Mg-rich primer and polyurethane top-coat system was applied onto AA2024-T3 substrates, and platinum circuit sensors were embedded between the primer and the topcoat. It was found that EIS in situ monitoring could be conducted with embedded sensors under constant immersion conditions. The two-electrode EIS configuration is suitable for tracking changes in open circuit potential. Electrochemical signal detected by the sensors tracks the response from the entire test specimen rather than localized areas of interest. However, this appears to be a limitation inherent to electrochemical impedance spectroscopy in general.

ACKNOWLEDGMENTS

This work was supported by the Air Force Office of Scientific Research under Grant No. FA9550-04-1-0368.

REFERENCES

1. O.O. Knudsen, U. Steinsmo, and M. Bjordal, Progress in Organic Coatings 2005, 54, 224-229.
2. EPA Federal Register 12.4, 60, No. 170, 1995, 45947.
3. D. Battocchi, D., Simo, A.M., Tallman, D.E. and Bierwagen, G.P., Corrosion Science 48, 2006, 1292–1306.
4. D. Battocchi, D., Simo, A.M., Tallman, D.E. and Bierwagen, G.P Corrosion Science 48 (2006) 2226–2240.
5. Nanna, M. E.; Bierwagen, G. P., JCT Research 2004, 1, 69-80.
6. Bierwagen, G. P.; Nanna, M. E.; Battocchi, D. Magnesium rich coatings and coating systems. 2004-US33089, 2005051551, 20041007. 2005.
7. Bierwagen, G.; Tallman, D.; Nanna, M.; Battocchi, D.; Stamness, A.; Gelling, V. J., Polymer Preprints (American Chemical Society, Division of Polymer Chemistry) 2004, 45, 144-145.
8. Bierwagen, G.; Battocchi, D.; Simoes, A.; Stamness, A.; Tallman, D., Progress in Organic Coatings 2007, 59, 172-178.
9. J. Kittel, N. Celati, M. Keddam, H. Takenouti, New methods for the study of organic coatings by EIS. New insights into attached and free films, Prog. Org. Coat., 2001, 41, 93.
10. J. Kittel, N. Celati, M. Keddam, H. Takenouti, Influence of the coating-substrate interactions on the corrosion protection: characterisation by impedance spectroscopy of the inner and outer parts of a coating, Prog. Org. Coat., 2003, 46, 135.
11. Miszcyk, T. Schauer, Electrochemical approach to evaluate the interlayer adhesion of organic coatings, Prog. Org. Coat., 2005, 52, 289.
12. K. N. Allahar, Quan Su, G. P. Bierwagen, D. Battocchi, V. J. Gelling, D.E. Tallman, Examination of the feasibility of the use of in-situ corrosion sensors in army vehicles, submitted to Proc. 2005 Tri-services Corrosion Conference, Orlando, FL 2005.
13. K. Allahar, Q. Su, G. Bierwagen, D. Battocchi, V. Gelling, D. Tallman, Further Studies of Embedded Electrodes for In-Situ Measurement of Corrosion Protective Properties of Organic Coatings, NACE Corrosion/2006 Conference, March 2006, San Diego CA.
14. K. Allahar, Quan, Su, G. P. Bierwagen, D. Battocchi, V. J. Gelling and D. Tallman, “Examination of the Feasibility of the Use of In-situ Corrosion Sensors in Army Vehicles”, 2005 Tri-service Corrosion Conference, Orlando, FL.
15. K. Allahar, Quan, Su, G. P. Bierwagen, “Monitoring of the AC-DC-AC Degradation of Organic Coatings by Embedded Sensors”, NACE Corrosion 2007 Conference, Nashville, TN.
16. M. Nanna and G. P. Bierwagen. Journal of Coatings Technology, April, 2004, 1, 52.
17. Impedance Spectroscopy, MacDonald, J.R., ed., Wiley-Interscience: New York, NY, p. 260-308, 1987.
18. Principles and Prevention of Corrosion, Jones, D.A., ed.; Macmillian Publ. Comp.: New York, NY, p. 122, 161, 1992.

FIGURES

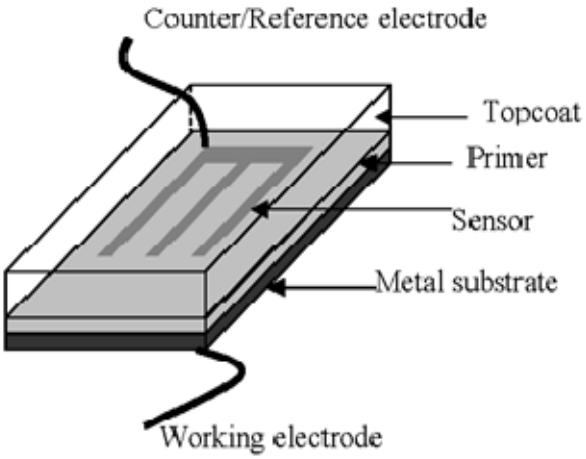

Figure 1. Schematic representation of an embedded sensor.

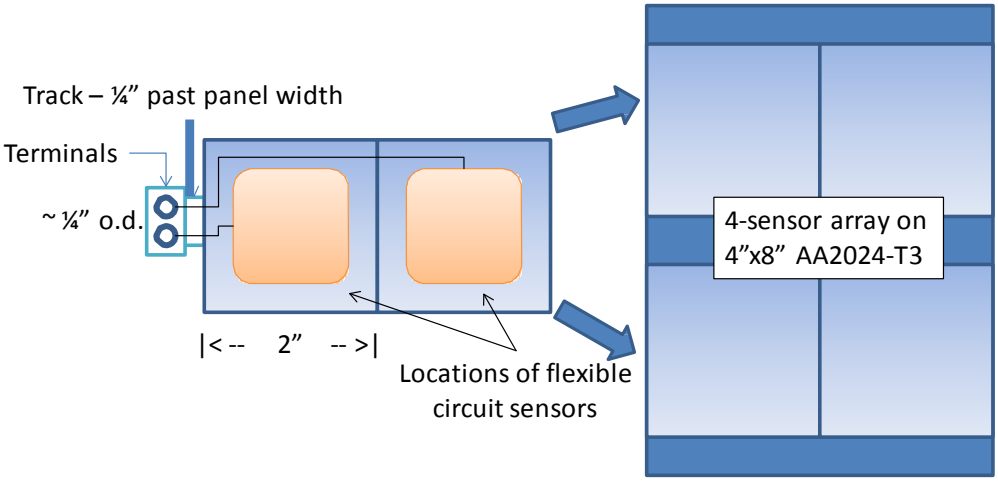

Figure 2. Arrangement of four circuit sensors on a test panel.

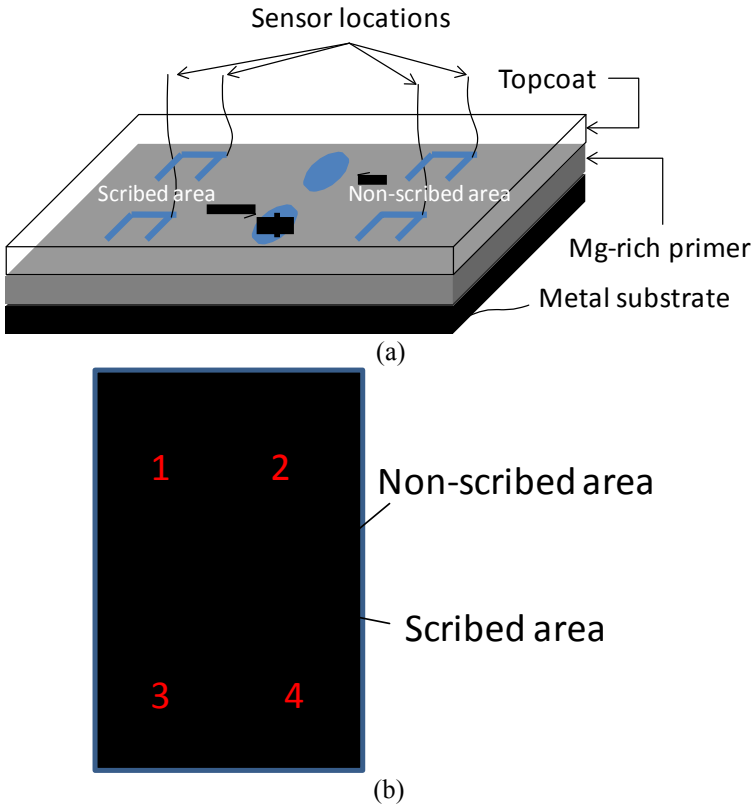

Figure 3. Experimental setup for in situ potentiostatic EIS and sensor identification.

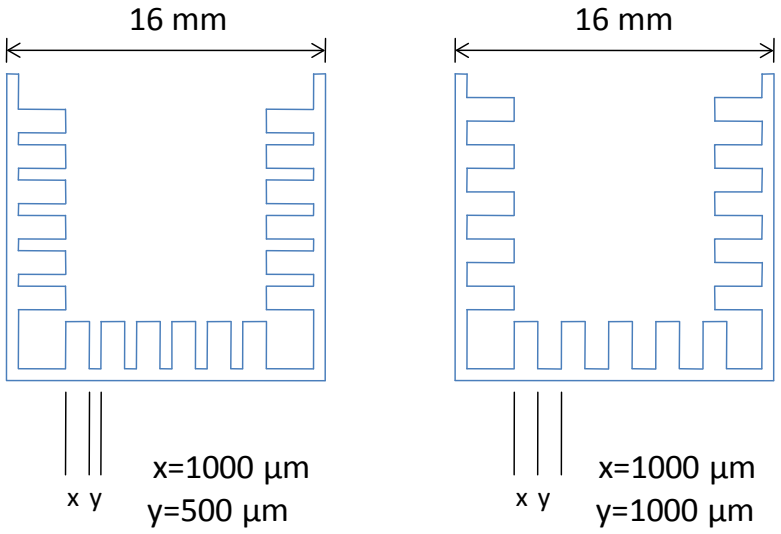

Figure 4. Circuit sensor design: geometry and dimensions.

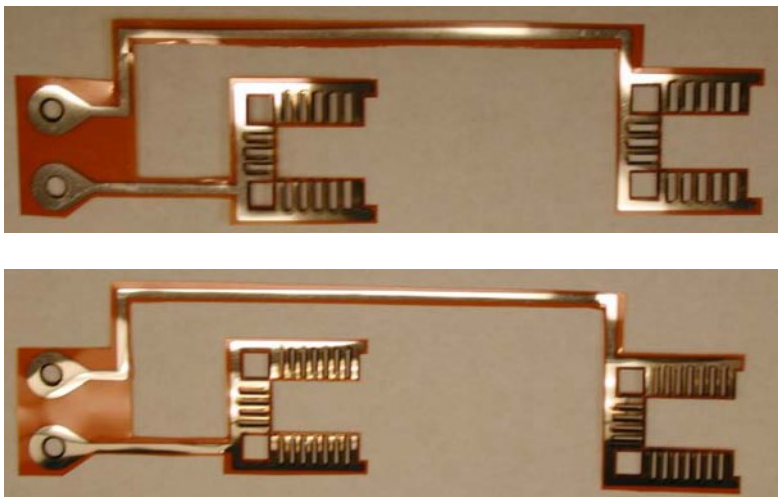

Figure 5. Circuit sensors before application to Mg-rich primer.

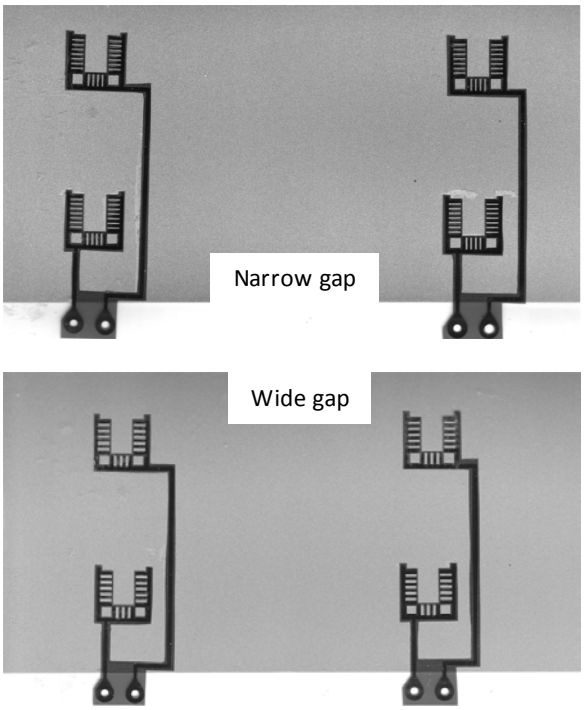

Figure 6. Sensors after application on top of Mg-rich primer.

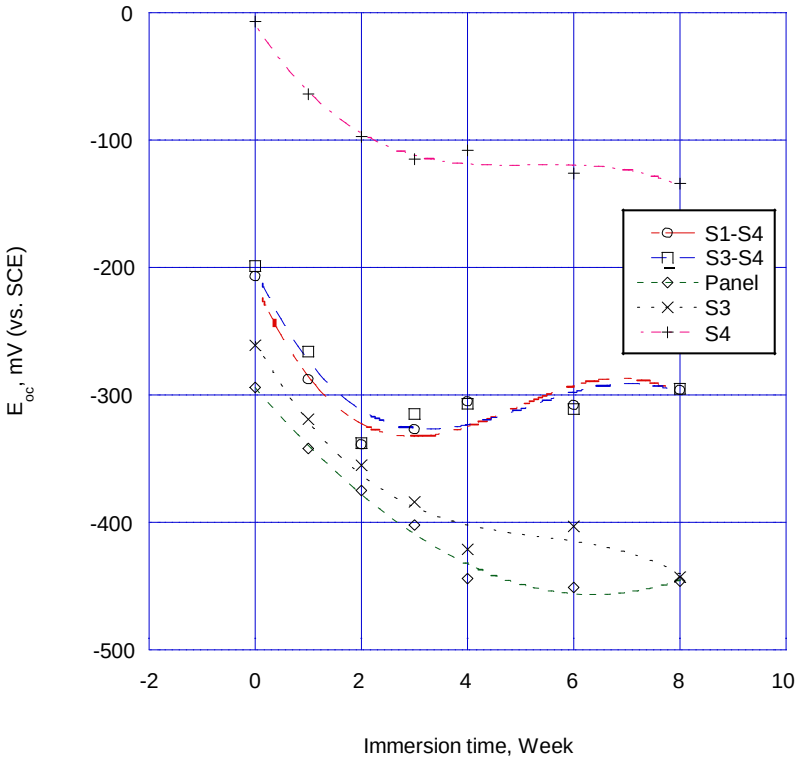

Figure 7. Open circuit potential for un-scribed sample.

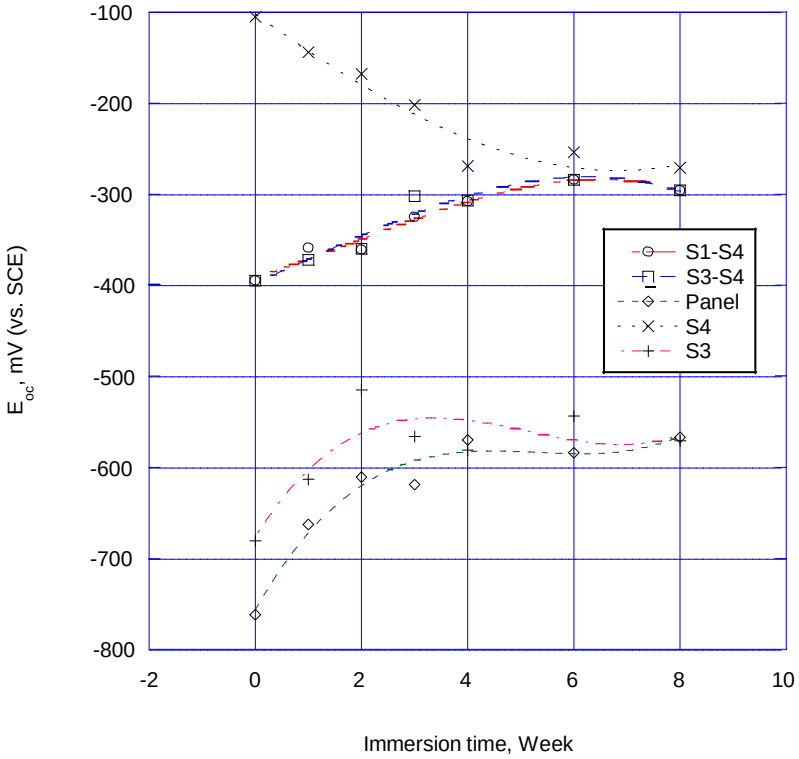

Figure 8. Open circuit potential for scribed sample.

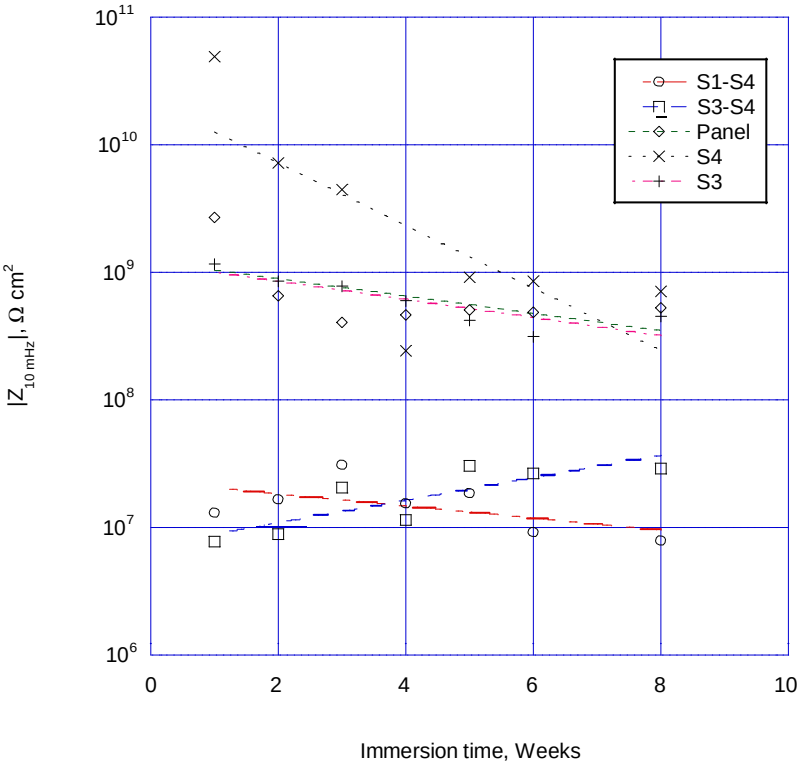

Figure 9. Low-frequency impedance modulus for un-scribed sample.

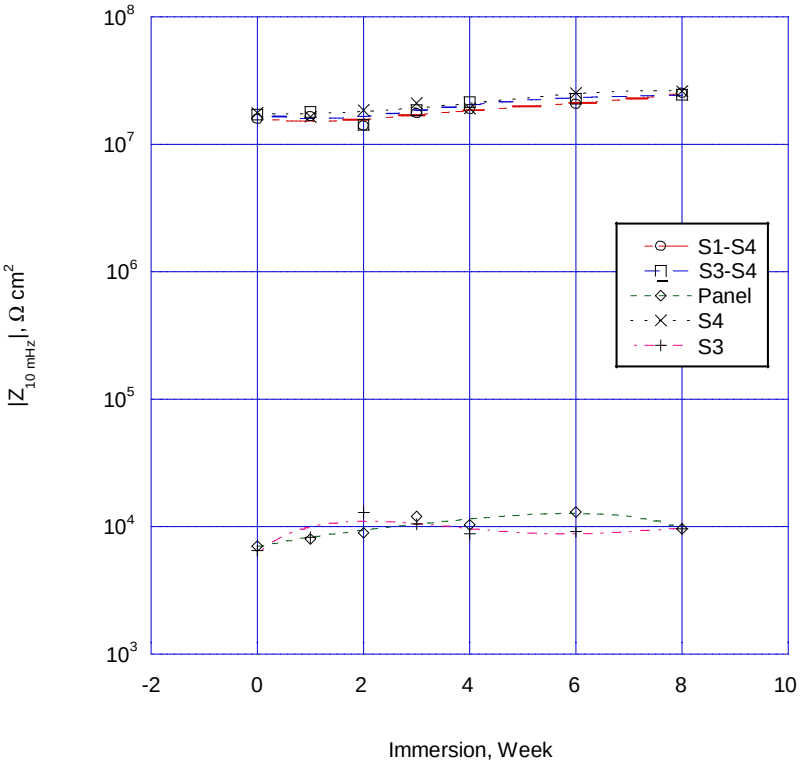

Figure 10. Low-frequency impedance modulus for scribed sample.

APPENDIX B

Corrosion Science 2011 (in press)

IN SITU MONITORING OF A MG-RICH PRIMER BENEATH A TOPCOAT EXPOSED TO PROHESION CONDITIONS

Duhua Wang,[1] Dante Battocchi,[1,2] Kerry N. Allahar,[1] Seva Balbyshev[3] and Gordon P. Bierwagen[1,2]

[1]Department of Coatings and Polymeric Materials

[2]Center for Surface Protection

[3]Center for Nanoscale Science and Engineering

NDSU Dept. 2760, P.O. Box 6050, Fargo, ND 58108-6050, USA

Ph: +1(701)231-6219

Authors e-mail: Duhua.Wang@ndsu.edu, Dante.Battocchi@ndsu.edu, Kerry.Allahar@ndsu.edu, Seva.Balbyshev@ndsu.edu, Gordon.Bierwagen@ndsu.edu

Abstract:

Mg-rich primers have been proven to be an adequate alternative for chromate-based coatings for the protection of aluminum alloys from corrosion. Their protection behavior was attributed to a combination of cathodic and barrier protection similar to the protection behavior associated with Zn-rich primers on steel substrates. The performance of a Mg-rich primer on aluminum 2024-T3 under Prohesion® exposure (ASTM G85) has been monitored using an embedded sensor placed at the surface of the primer and below the topcoat. The accelerated weathering cycle simulates outdoor weather exposure by alternating wet and dry steps. Electrochemical impedance spectroscopy (EIS) and noise measurements (ENM) were conducted to monitor the performance and the electrochemical properties of the system beneath the topcoat. The data analysis demonstrates that the sensor is able to detect change in the barrier properties of the topcoat in response to the exposure conditions and the activation of the pigments in the primer in the presence of electrolyte.

Keywords: Mg-rich primer, embedded electrodes, EIS, ENM

INTRODUCTION

Corrosion protection by coatings is mainly based on the combination of binders (polymer resins) and pigments. For epoxy esters, drying oils and phenolic epoxy paints, the corrosion protection is mainly attributed to the barrier properties from binders, which can reduce the transport of water, ions, and oxygen from the environment to the substrate [1-3]. On the other hand, in red lead, zinc chromate yellows and

zinc-rich primers, the pigments' inhibition, passivation, and cathodic protection are the main causes for reducing corrosion.

Corrosion is a natural process and the accelerated weathering, such as Prohesion® and salt spray exposure, aims to reproduce and accelerate natural corrosion and degradation processes of the coating system and the substrate without changing the corrosion/degradation mechanism as occurs in practice. The most often used accelerated test is the salt spray test, which involves continuous spraying of 5% sodium chloride (NaCl) in distilled water at 35°C [2]. It can be performed in accordance with ASTM B117, ISO 7253, ISO 9227, DIN 53167, or BS 3900. Salt spray was first used for corrosion testing around 1914. In 1939, the neutral salt spray test was standardized in ASTM B117. However, cyclic corrosion test results generally correlate better with natural corrosion than salt spray test results do. This is pointed out in many of the references [4-9]. The first cyclic test, the so-called Prohesion test, was developed in the UK in the 1970s. It is covered since 1994 in an annex of ASTM G85, together with other modifications to the basic salt spray test. A typical Prohesion test includes a fog/wet step of 1 hour salt spray at 25^{o}C and a dry step of 1 hour hot air at 35^{o}C. Dilute Harrison's solution (0.05 wt% NaCl and 0.35 wt%t $(NH_4)_2S0_4$ at pH=5.0-5.4) is used as the salt fog solution in the Prohesion chamber. Accelerated weathering cannot replicate the real natural corrosion process. G. Gardner pointed out that continuous salt spray accentuated blistering and that cyclic salt spray emphasized filiform and undercut corrosion [4]. Because of the problems inherent in exposure testing methods, especially their subjective nature, quantitative electrochemical testing has become a widely used alternative [10]. The major electrochemical test methods used for examining the coatings systems and metal pretreatments are electrochemical impedance spectroscopy (EIS), electrochemical noise methods (ENM), and potentiodynamic scanning (PDS). [10-15].

A technique for in-situ monitoring of coatings involves an embedded electrode sensor within a coating system. The Department of Coatings and Polymeric Materials at NDSU has been at the forefront in the development and application of embedded sensors, which consist of electrodes that act as the counter and reference electrode, but are placed between the layers of a two-layer coating system [16, 17]. The major advantage of this sensor application is that the electro-chemical measurement of the primer/metal interface can be made without being masked by high resistance topcoat. Until now, the embedded sensors approach has been applied for characterization of standard Air Force and Army vehicle coatings that are evaluated by thermal cycling accelerated testing method [18], and accelerated ac-dc-ac testing method. [19] While there have been limited studies published on the use of embedded sensors in the aforementioned coating systems, there has been no application to metal rich primers, e.g. Mg- or Zn-rich primers. By analogy to the formulation of zinc-rich primers for the protection of steel, magnesium–rich, pigmented primers are now being formulated for the protection of aluminum alloys. This work motivated by the need for chromate-free alternatives for protection of high-strength aircraft Al alloys such as 2024-T3 and 7075-T6. G.P. Bierwagen and the corrosion group at NDSU are leading this Mg-rich primers research and a series of articles have been published [20-22] on their application and properties. The coupling of embedded sensors and coating

systems with Mg-rich primers is a unique approach that allows in-situ monitoring of the electrochemical behavior of protective Mg-rich primers beneath a topcoat.

EXPERIMENTAL

The protective coating system used in the experimental procedure was composed of a high solids polyurethane clear topcoat (AKZO NOBEL 646-58-7925CLEAR) and a Mg-rich primer developed at NDSU [20]. In this primer, Mg powder with the average particle size of 25 μm (Ecka Granules of America, Louisville, KY) was dispersed in a two-component epoxy-polyamide resin, and the pigment volume concentration (PVC) of the primer was 45%. The primer was applied to standard panels of aluminum alloy 2024-T3. After the application of the primer, a platinum sensor was applied on the surface of the primer, followed by the application of the polyurethane topcoat. The embedded sensor was between the primer and the topcoat for each of the final coated panels. Using the same method, the embedded sensor was placed between the primer and the topcoat of all coated panels.

Sample Preparation

The aluminum alloy 2024-T3 panels were polished by 200 grit followed by 600 grit sanding paper, then washed with hexane and dried with a nitrogen flow. The freshly pretreated metal panels were coated within half an hour after they were polished.

The sensor was made from platinum leaves obtained from Wrights of Lymm Ltd, Manchester, England, and was approximately 130 nm thin. Supported by tissue paper, the platinum leaf was cut into the designed sensor shape with the surface area of the sensor being 2.56 cm^2 and the width of each side 0.4 cm as shown in Figure 1 with the sensor on the surface of the Mg-rich primer and covered by a polyurethane clear topcoat.

The sensor was adhered to the primer by applying a thin layer of a homemade epoxy resin (D.E.R. 331 epoxy resin/Ancamide 2353/methyl ethyl ketone at a 5/3/5 weight ratio) to the surface of the primer. The platinum sensor was then placed on this epoxy resin and adhered onto the primer after 10 minutes of solvent flash-off and cured. A copper core insulated wire was soldered onto the embedded sensor. The same epoxy resin (D.E.R. 331) was used to seal the conducting joint and given one day to harden at room temperature before the polyurethane topcoat was applied. The approximate neat dry film thickness of Mg-rich primer was 50 μm, and 40 μm for the topcoat.

The exposure of the panels in the Prohesion chamber required that the back and the edges of the coated panel be isolated from the environment. This was done by spraying the same coating system, Mg-rich primer and polyurethane clear topcoat, to the back of the panel. The edges of the panels were dip-coated with the same coating system.

Experimental Configurations

The in-situ monitoring of the Mg-rich primer + polyurethane clear topcoat was carried out under Prohesion exposure condition. A Gamry PCI4-300 was used for the potentiostatic EIS measurements with a frequency range from 100 kHz to 0.05 Hz and a perturbation potential of 15 mV RMS. A data acquisition rate of 10 points per decade was employed. The two-electrode (2E) EIS method (sensor-substrate) was used to obtain the EIS responses in a one-panel setup, where a coated panel was assembled with two sensors placed approximately 8 cm apart. As shown in the schematic diagram in Figure 1, the working electrode was connected to the metal substrate and the reference and counter electrodes were connected to the embedded sensor.

Another 2E EIS setup (sensor-sensor) consisted of one sensor connected to the working electrode and the other sensor connected to the counter and reference electrodes, as show in Figure 1.

The fast data acquisition mode was used in both two-electrode EIS measurements, and frequency scans from 100 kHz to 0.05 Hz took about 12-15 minutes. The single frequency impedance measurement was also carried out using the sensor-to-sensor 2E configuration at the frequency of 10 kHz.

The configuration for the ENM measurement is shown in Figure 1. A one-panel/two sensor setup was utilized, where the two sensors acted as working electrodes and the substrate was the reference electrode. Experiments was carried out in zero resistance ammeter (ZRA) mode on a Gamry PCI4/300 potentiostat (Gamry Instruments, Inc. of Warminster, PA) coupled with Gamry ESA400 software (ver. 4.21), with the data acquisition frequency of 5 Hz. This configuration is theoretically the same as the traditional ENM three-electrode configuration [23], involving a reference electrode and two coated panels acting as two separate working electrodes electrically connected via a salt bridge. It has been shown that similar information can obtained from both the traditional and present configurations [23,24].

Testing Procedure

In order to achieve total curing, tested panels were placed under ambient conditions for at least 10 days before being placed into the Prohesion chamber. The electrical leads for the embedded sensor and the

substrate were long enough to connect each panel with the potentiostat and computer located outside the chamber. After a certain period of exposure in the Prohesion chamber, EIS experiments were carried out using the two-electrode configurations during both dry and wet steps of the Prohesion protocol, followed by the ENM testing typically consisting of 3 cycles of dry and wet steps of the Prohesion test.

During the first three weeks in Prohesion chamber, EIS and ENM testing were carried out every day. After three weeks, electrochemical measurements were carried out every other day. The total duration of this experiment was 60 days.

The EIS experiments were conducted in both the dry and wet steps after 30 minutes once the chamber environment has stabilized and the coating surface has reached either dry or wet condition, respectively. Additional experiments were also conducted to characterize the behavior of the Mg-rich primer during the changing environmental conditions. A single frequency experiment was conducted every other week during Prohesion exposure to characterize the capacitance behavior of the primer. This experiment involved measurement of the impedance at an applied frequency of 10 kHz over a period of time, typically 3 cycles. In addition, the temperature of the coating surface was monitored using thermocouple sensors for several early cycles of Prohesion exposure.

RESULTS AND DISCUSSION

Chamber Temperature and Coating Capacitance Study

Electrochemical impedance measurements require steady state conditions during the data acquisition process. The environmental conditions in the Prohesion chamber changed rapidly with time. In order to conduct in-situ EIS measurements on the coated panels in the Prohesion chamber, a relatively stable state should be identified first. The changes of temperature and the capacitance associated with the measured panels were investigated, and the influence of Prohesion conditions on coating electrical properties was studied. Based on these findings, a proper time range was identified for the EIS test.

The temperature profile at the surface of a coated panel was measured during an early Prohesion cycle and is shown in Figure 2. The 1-hour exposure of a dry step exhibited a temperature increase from 25^{o}C to 45^{o}C in 20 minutes, followed by a drop to 40^{o}C over the next 40 minutes. The 1-hour exposure of the wet (fog) step included a drop from 40^{o}C to 27^{o}C over the first 55 minutes with a subsequent drop to 25^{o}C over the last 5 minutes.

The relative dielectric permittivity of water at room temperature is approximately 80, while that of an epoxy polymer is in the range of 3 to 5. The ingress of water into a coating is associated with an increase of the dielectric constant of the coating with a concomitant increase of coating's capacitance [25,26]. The evolution of the coating's impedance at high frequency (10 kHz) was measured during the dry and wet steps of the Prohesion cycle. The impedance data were used to calculate the capacitance of the coating, C_c, using:

$$C_c = -1 / (2 \pi f Z'')$$

where f is the frequency and Z'' is the imaginary component of impedance.

The evolution of the calculated coating capacitance after 16 days of Prohesion exposure is shown in Figure 2. In the dry step, the capacitance value clearly had a profile resembling the temperature fluctuations. The capacitance increased from 0.30 nF to 0.35 nF during the first 35 minutes of the dry step and decreased to the lowest point of ~0.28 nF during the first several minutes of wet cycle. It appears that the temperature factor dominated the changes of capacitance in the dry step. With the temperature increasing, the polyurethane topcoat became more porous and thus more prone to water ingress. Conversely, it provided better barrier to moisture when the temperature decreased. In the wet step, the capacitance was maintained around 0.30 nF, most likely due to the combination of the fog spraying environment and decreasing temperature in the wet step. Overall, the capacitance changes were attributed more to the temperature changes during the dry and wet steps in Prohesion exposure. It was also found that the environmental conditions in Prohesion chamber varied all the time and the electrochemical impedance data were affected by the different chamber conditions. In order to have an effective analysis and comparison of data, we chose to present and plot the EIS data collected during the 40-50 minute range in dry and wet steps.

Open circuit potential (OCP)

The open circuit potential is a very important parameter for monitoring the behavior of metal- rich coatings. The OCP time records presented in Figure 3 were measured in-situ with the embedded sensors and ex-situ with a conventional 3 electrode setup. In this case, the embedded sensor and the ex-situ recorded values present a difference of ca. 400 mV, the embedded sensors values being more positive of the two.

EIS Results

Sensor-substrate EIS

Two-electrode EIS method (sensor-substrate) was used to obtain the EIS responses (Figure 1). EIS measurements for the frequency range of 100 kHz to 0.05 Hz were performed after 40 minutes of drying and wetting, respectively. Total duration of testing was 60 days when the coatings failed both by visual inspection and electrochemical testing. The EIS Bode plots during the Prohesion dry and wet steps are shown in Figure 4, as a function of exposure time. It was observed that the |Z| spectra almost superimposed in the 100 Hz to 100 kHz high-frequency range up to 20 days of Prohesion exposure,. This suggested that the capacitance of the coating was approximately the same at the end of 20-day Prohesion chamber exposure. After 20 days, the high frequency value of |Z| decreased with time. The impedance in the mid-frequency range of 1Hz to 100 Hz was scattered for about 10 days, with the scatter becoming negligible as the time elapsed. The |Z| modulus value in the low frequency range of 0.05 Hz to 1 Hz was continuously decreasing until 43 days of chamber exposure. It was found that the |Z| data for days 43 and 60 almost overlapped, in both the dry and wet steps. There were plateau regions in the 0.05 Hz to 100 Hz frequency range during the Prohesion exposure, which are indicative of the barrier properties provided by the surface coating, in this case, by the polyurethane clear topcoat, since the Mg-rich primer usually contributes to cathodic protection and shows a lower impedance, $< 10^6\ \Omega$ [20,21].

Barrier property is a major characteristic of corrosion protective coatings. Barrier property of a coating can be gauged by the resistance of the coating to the passage of electric current. For this reason, the low-frequency modulus value has been widely used as an estimate of coating's barrier properties [27,28]. In this study, the |Z| value associated with the frequency of 0.05 Hz was used as an estimate of the barrier property of the coating. The $|Z|_{0.05\ Hz}$ values for both the Prohesion dry and wet steps as a function of exposure time are shown in Figure 5. It was found that both $|Z|_{0.05\ Hz}$ values for dry and wet steps had similar profiles for the first 10 days, indicative of rapid decrease of the modulus from about $1x10^9\ \Omega$ to$1x10^8\ \Omega$. At the 10-day mark, the wet $|Z|_{0.05\ Hz}$ values dipped to around $1x10^8\ \Omega$, followed by another rapid decrease to $4x10^6\ \Omega$ during the 20–40 day period. After about 40 days, the $|Z|_{0.05\ Hz}$ values stabilized around $3x10^6\ \Omega$ for the duration of the testing. The dry $|Z|_{0.05\ Hz}$ values showed similar changes with about $1x10^7\ \Omega$ during the first 10-20 days, followed by a rapid drop to $1x10^6\ \Omega$ by day 40 and no further change for the remainder the test. It was clearly observed that the barrier properties of the coatings were weakened step by step during the 60 days' Prohesion chamber exposure. Another finding was the wet $|Z|_{0.05\ Hz}$ values being relatively higher than the dry ones, that may due to the higher average temperature in the dry step (Figure 2) and the fact that the polyurethane topcoat is more sensitive to higher temperature due to its porosity.

The capacitance values C_c, calculated from the impedance data at the frequency of 9998.2 Hz, were plotted as a function of time in Prohesion chamber (Figure 6). The trends in the C_c values were similar for the dry and wet conditions, increasing from 0.1 to 0.2 nF for the first 20 days, then quickly increasing from 0.2 to 0.7 nF for another 20 days, reaching over 1 nF after day 50. These results indicated that barrier properties of the coating during the Prohesion exposure decreased slowly in the beginning, then weakened quickly after 20 days. This change pattern was found to be consistent with the EIS Bode plots and $|Z|_{0.05\ Hz}$ values. All the results showed that the coatings started to degrade from the beginning of the Prohesion exposure and failed to provide to barrier properties after about 40 days of Prohesion exposure.

Sensor-sensor EIS

In addition to the two-electrode (2E) sensor-substrate EIS method, sensor-sensor EIS measurement (Figure 1) was used for in-situ monitoring of the coating system changes during the Prohesion exposure. Theoretically, |Z| values from the sensor-sensor EIS measurement should be the complex of the two |Z| values from individual sensors, so the EIS data from the sensor-sensor configuration should be very similar to those acquired with the sensor-substrate EIS setup.

Sensor-sensor EIS measurements for the frequency range of 100 kHz to 0.05 Hz were performed after 40 minutes into the drying and wetting steps,. The first testing day was day 14 of Prohesion exposure and final day of 2E sensor-sensor EIS testing was day 60. The EIS Bode plots for the Prohesion dry steps are shown in Figure 10 as a function of exposure time. It was observed that the impedance response had slight changes from day 14 to day 21, and the low- frequency impedance on day 30 was around $1x10^7\ \Omega$. The |Z| value for days 43, 52 and 60 were almost superimposed throughout the entire frequency range, and the low frequency modulus values were down to about $1x10^6\ \Omega$. The phase angles prior to day 30 were close to -80° in the high frequency range, which was indicative of coatings performing like a capacitor. Phase angles after day 43 were about -60° in the 100 Hz to 100 kHz high-frequency range. All the phase angles were around -30° in the 0.05 Hz to 1 Hz range, indicating the barrier properties of coatings were decreasing. The EIS Bode plots during the Prohesion wet steps had the very similar profiles.

Figure 8 shows the changes of low frequency modulus $|Z|_{0.05\ Hz}$ values as the function of Prohesion exposure time. Both $|Z|_{0.05\ Hz}$ values of dry and wet steps had similar change patterns, involving gradual decrease from about $1x10^8$ to $8x10^6\ \Omega$ for the wet step and from $2x10^7$ to $1x10^6\ \Omega$ for the dry step between days 14 and 43, followed by no changes in the modulus values up until the end of testing on day 60. It is

apparent that the coatings were failing and losing barrier properties during Prohesion exposure. It was also found that the $|Z|_{0.05\ Hz}$ values of wet steps were higher than those of dry steps. This result is consistent with the findings of the sensor-substrate EIS.

The capacitance values C_c were plotted as a function of Prohesion exposure time (Figure 9). C_c values both from dry and wet steps were increasing with time from about 0.2 nF to over 1 nF, indicating that the coatings were more susceptible to absorbing moisture and losing barrier properties.

Single Frequency Capacitance

As mentioned before, the increasing capacitance of a coating means the increasing of the dielectric property and more accessible to water uptaking of a coating. The classic Brasher-Kingsbury equation [29] can be used to quantitatively calculate the volume percentage of absorbed water (< 5%) in a coating film. A large coating capacitance value always represents more chance for water to get into the film. In this study, the evolution of the impedance of the coating at 9998.2 Hz on different Prohesion exposure days was measured during 3 dry and wet cycles, for a total of 6 hours. Capacitance values at 9998.2 Hz, $C_{9998.2Hz}$. were calculated from the impedance data and are shown in Figure 10. The $C_{9998.2Hz}$ evolution pattern varied with the Prohesion chamber conditions: capacitance values fluctuated in the dry step and remained relatively unchanged in the wet step. This was most likely due to the specific polyurethane clear topcoat being very sensitive to the temperature changes in the Prohesion chamber dry step. The dry step temperature increased from 25°C to 45°C for the first 20 minutes, then remained constant for the most part of the test and slightly decreased to about 40°C at the end of the dry step. In the dry step, topcoat was softened and thus more accessible to moisture penetration with the increasing temperature, while providing better barrier to electrolyte when the temperature decreased. In the wet step that follows the dry step, on the one hand, the temperature continues to decrease from 40°C to 25°C, but on the other hand, the fog fills up the entire chamber. This combination of decreasing temperature and the wetting atmosphere in the chamber keep the capacitance of the coating relatively constant. As expected, the capacitance levels were increasing with longer exposure times. The $C_{9998.2Hz}$ values for day 16 were in the 0.25-0.35 nF range, while the $C_{9998.2Hz}$ values from day 51 fluctuated much more, between 1.0 and 1.5 nF. Clearly, the longer the exposure in Prohesion chamber, the higher and more fluctuated the values of $C_{9998.2Hz}$ were, indicating that the coating's barrier properties were deteriorated during Prohesion exposure.

ENM Results

Electrochemical noise measurements were conducted while the coated panels were exposed in the Prohesion chamber. Both the electrochemical potential and current noise records were collected. The

ENM monitoring was carried out continuously for more than 6 hours, which covered three dry-wet Prohesion cycles.

The original ENM raw data are not reported here directly, due to the overwhelming amount of date points. Instead, the noise resistance (R_n) value is discussed. R_n was obtained by dividing the standard deviation of the potential noise by the standard deviation of the current noise. In fact, the original potential and current raw noise data were divided into many small blocks, each containing 128 data points, which is equivalent to 25.6 seconds of testing period. Linear detrending was also applied to the original noise data of each block to remove the electrochemical drift, and then noise resistance was calculated [30]. Therefore, the R_n values reported here are, in fact, averages over 128 data points (25.6 seconds).

It has been reported elsewhere that R_n is quantitatively close to the coating polarization resistance R_p and the low frequency impedance modulus, and thus can serve as a good indicator of the barrier properties and lifetime prediction of coating performance [31-32]. The R_n values for three different days of Prohesion exposure are shown in Figure 11. For day 1, the R_n values were constant in the dry step and slightly scattered in the wet step, but all close to $1x10^9$ Ω, showing that the coating film acted as a good barrier at the early stage of Prohesion exposure. After 10 days, much more scattered values from 10^7 to 10^9 Ω were observed for both the dry and wet steps, and the averaging R_n value was around 10^8 Ω, indicating that the coating still provided adequate barrier protection. However, there was no obvious difference in terms of magnitude and dispersibility of the R_n values in dry and wet steps. It means that once the coatings started to degrade, the water and electrolyte absorbed onto the coating surface could not be totally driven out during the dry step or that the coating had been softened in the dry step and rendered more accessible to moisture. The Rn values were only between 10^4 to 10^6 Ω after 60 days of Prohesion exposure, indicating fairly low barrier properties afforded by the coating towards the end of the test, at which point the film could be easily wetted allowing the electrolyte to penetrate further into the primer and to the substrate/primer surface.

It was observed from Figure 10 that the R_n values varied significantly between the first day and the last days of data acquisition. In order to better illustrate the evolution of the noise resistance of the coating system, R_n values from both dry and wet steps were plotted as a function of Prohesion exposure time, as shown in Figure 12. Here, the R_n values are average noise resistance values from 30 to 45 minutes into either dry or wet steps.

The R_n started from very high values, $1x10^9\ \Omega$, then quickly dropped to $1x10^7\ \Omega$ after about 10 days and maintained that value for another two weeks, followed by another quick drop to $1x10^6\ \Omega$ after about 6 weeks of Prohesion exposure, and eventually leveled off for the rest of the test. This R_n value profile was highly consistent with the evolution of the low-frequency impedance modulus from EIS, indicating that both EIS and ENM techniques when combined with sensors can detect the coating changes during the entire Prohesion exposure were found in good correlation with each other.

CONCLUSIONS

The Mg-rich primer and polyurethane clear topcoat system was applied onto AA2024-T3 substrates, and platinum sensors were embedded between the primer and the topcoat. Then the coated substrates were put into the standardized Prohesion chamber to simulate weathering conditions in an aggressive manner to induce accelerated coating failure. The acquisition of EIS and ENM data from embedded sensor in-situ monitoring during the Prohesion dry and wet steps provided insight into the coating behavior evolution. It was found that both EIS and ENM in-situ monitoring could be conducted with embedded sensors under both dry and wet Prohesion steps. Under the dry Prohesion step, the coatings were sensitive to the temperature changes, while in the wet step, the resistance values were more scattered due to the moisture accumulation on the coating surface. The effects of both the temperature and humidity variation on changes in coating propertiess were in-situ monitored by the embedded sensors in Prohesion chamber. It was found that the coating degraded continuously with Prohesion exposure time as evidenced by the gradual decrease of both low frequency impedance $|Z|_{0.05\ Hz}$ and noise resistance R_n.

ACKNOWLEDGMENTS

This work was supported by the Air Force Office of Scientific Research under Grant No. FA9550-04-1-0368.

REFERENCES

1. Z. W. Wicks, F. N. Jones and S. P. Pappas. *Organic Coatings Science and Technology*, Second Edition. **1998**, 129-140.

2. G. P. Bierwagen, *Progress in Organic Coatings,* **1996,** 28, 43..

3. Ray Mudd, *Journal of Protective Coatings & Linings,* October **1995,** 51.

4. G. Gardner, "ASTM's New Coating Test Method Addresses Interactive Effects of Weathering and Corrosion," *Journal of Protective Coatings & Linings,* September **1998,** 50.

5. G. Gardner, "Recently Developed ASTM Test Addresses Interactive Effects of Weathering and Corrosion," *Protective Coatings Europe,* February, **1999**, 86.

6. Van Leeuwen, *Protective Coatings Europe*, January, **1996**, 42.

7. C. Simpson and R. C. D. Hicks, "ASTM D5894 and the Development of Corrosion Resistant Coatings," *Paint & Coatings Industry*, May, **1997**, 76.

8. N. D. Cremer, *Polymers Paint Colour Journal*, **1998**, 188, 31.

9. S. L. Chong, *Journal of Protective Coatings & Linings,* March, **1997**, 20.

10. B. S. Skerry and D. A. Eden, *Progress in Organic Coatings*, **1987**, 15, 269.

11. C. H. Tsai and F. Mansfeld, "Determination of Coating Deterioration with EIS. Part II. Development of a Method for Field Testing of Protective Coatings," *Corrosion*, **1993**, 49, 726.

12. F. M. Greenen, J. H. W. DeWit and E. P. M. Van Westing, *Progress in Organic Coatings*, **1990**, 18, 299.

13. D. Loveday, P. Peterson and B. Rogers-Gamry Instruments "Evaluation of organic coatings with Electrochemical Impedance Spectroscopy, part 2: Applications of EIS to coatings" *J. Coat. Technol.*, October, **2004**, 88.

14. D. A. Eden, M. Hoffman and B. S. Skerry, Application of electrochemical noise measurements to coated systems, in: R.A. Dicke, F.L. Floyd (Eds.), Polymeric Materials for Corrosion Control, ACS Symposium Series 322, American Chemical Society, Washington, DC **1986**.

15. M. Selvaraj and S. Guruviah, *Progress in Organic Coatings*, **1996**, 28, 271.

16. G. P. Bierwagen, X. Wang and D. E. Tallman, "In-situ Study of Coatings Using Embedded Electrodes for ENM Measurements", *Progress in Organic Coatings*, **2003**, 46, 163.

17. K. Allahar, Quan, Su, G. P.Bierwagen, D. Battocchi, V. J. Gelling and D. Tallman, "Future Studies of Embedded Electrodes for In-situ Measurement of Corrosion Protective Properties of Organic Coatings," NACE Corrosion/2006 Conference, March **2006**, San Diego CA.

18. K. Allahar, Quan, Su, G. P. Bierwagen, D. Battocchi, V. J. Gelling and D. Tallman, "Examination of the Feasibility of the Use of In-situ Corrosion Sensors in Army Vehicles", **2005** Tri-service Corrosion Conference, Orlando, FL.

19. K. Allahar, Quan, Su, G. P. Bierwagen, "Monitoring of the AC-DC-AC Degradation of Organic Coatings by Embedded Sensors", NACE Corrosion **2007** Conference, Nashville, TN.

20. M. Nanna and G. P. Bierwagen. *Journal of Coatings Technology*, April, **2004**, 1, 52.

21. D. Battocchi and G. P. Bierwagen. *Corrosion Science*, **2006**, 48, 1292.

22. D. Battocchi and G. P. Bierwagen. *Corrosion Science*, **2006**, 48, 2226.

23. X. Wang, "Study on novel electrode configurations for in situ corrosion monitoring on coated metal systems", Ph.D. Thesis, Chapter 3, Faculty of Science and Mathematics, North Dakota State University, **2002.**

24. S. Mabbutt, D.J. Mills, Surf. Coat. Int. Part B: *Coat. Trans.*, **2001**, 84, 277

25. R. A. Cottis, *Corrosion*, **2001**, 57, 265

26. H. A .A. Al-Mazeedi and R. A. Cottis, *Electrochim. Acta*, **2004**, 49, 2787

27. H. K. Yasuda, C. M. Reddy, Q. S. Yu, J. E. Deffeyes, G. P. Bierwagen and L. He, *Corrosion*, **2001**, 57, 29

28. J. N. Murray, *Progress in Organic Coatings*, **1997**, 31, 375

29. D. M. Brasher and A. H. Kingsbury, *Journal of Applied Chemistry*, **1954**, 4, 62.

30. R. A. Cottis, *Corrosion*, **2001**, 57, 265.

31. D. J. Mills and S. Mabbutt, *Progress in Organic Coatings*, **2000**, 39, 41.

32. G. P. Bierwagen, C. S. Jeffcoate, J. Li, S. Balbyshev, D. E. Tallman and D.J. Mills, *Progress in Organic Coatings*, **1996**, 29, 21.

FIGURES

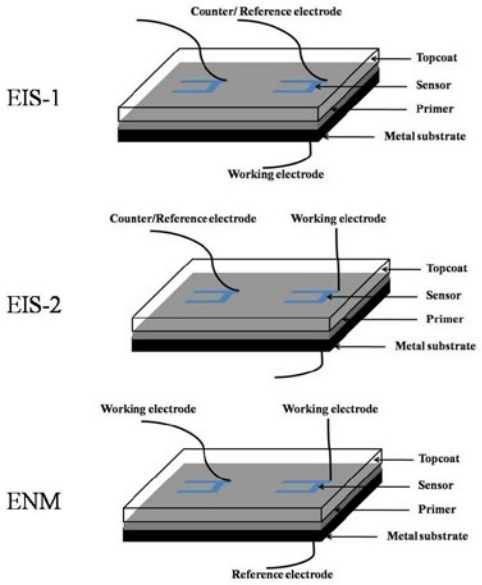

Figure 1. Schematic diagram of the electrochemical experimental setup. EIS-1: Sensor-substrate EIS, where the embedded sensor is the reference/counter electrode and the substrate is the working electrode. EIS-2: Sensor-sensor EIS, where one embedded sensor serves as the reference/counter electrode and the other as the working electrode. ENM: where the embedded sensors serve as working electrodes and the substrate is the reference electrode.

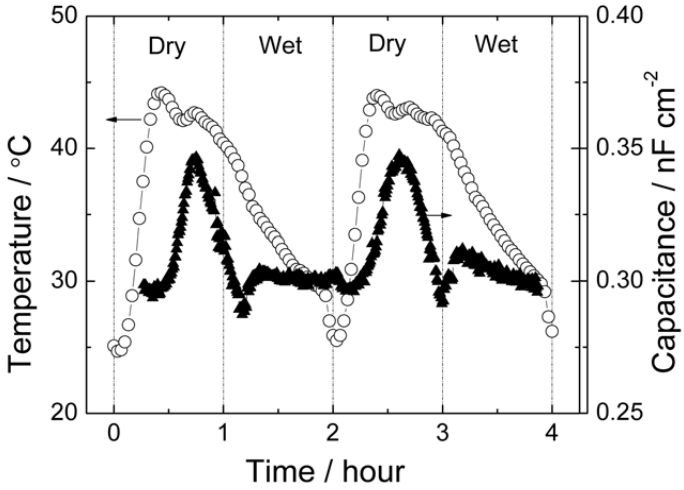

Figure 2. The temperature profile at the surface of the coated panel and the calculated capacitance during the dry and wet steps of Prohesion conditions. Dashed lined are used to identify the steps.

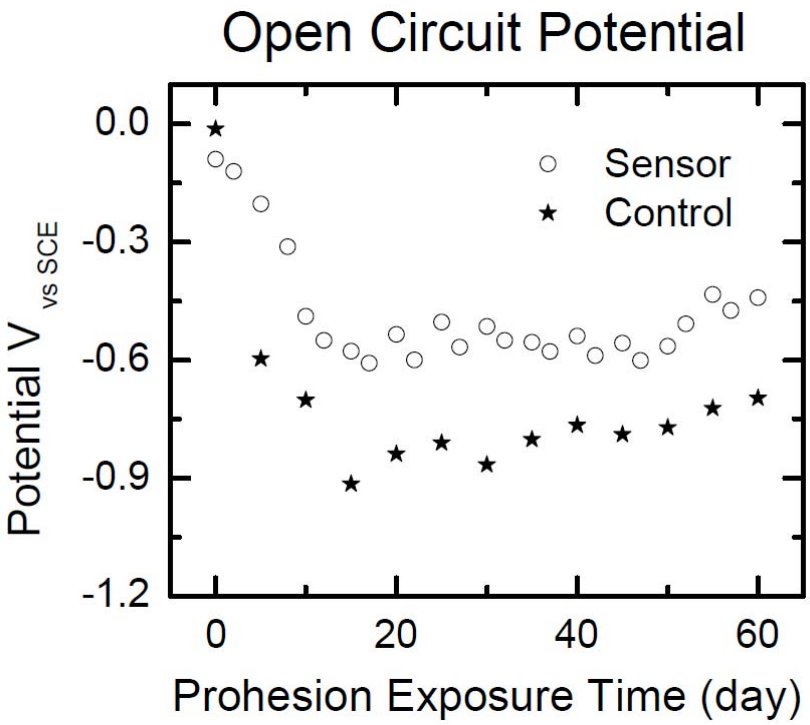

Figure 3. OCP monitoring in-situ (sensor) and ex-situ (control, 3E setup).

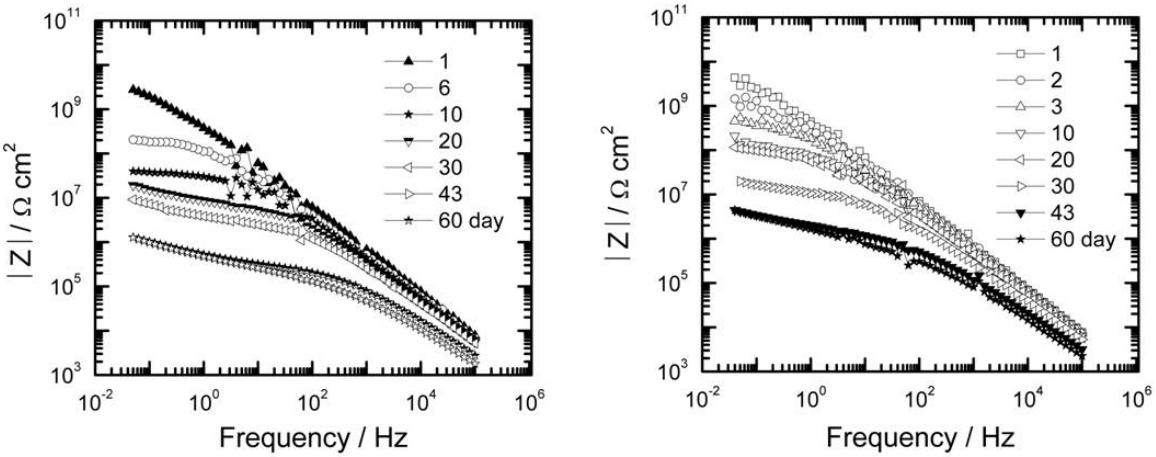

Figure 4. Impedance of sensor-substrate EIS data during the Prohesion dry steps (left) and wet steps (right).

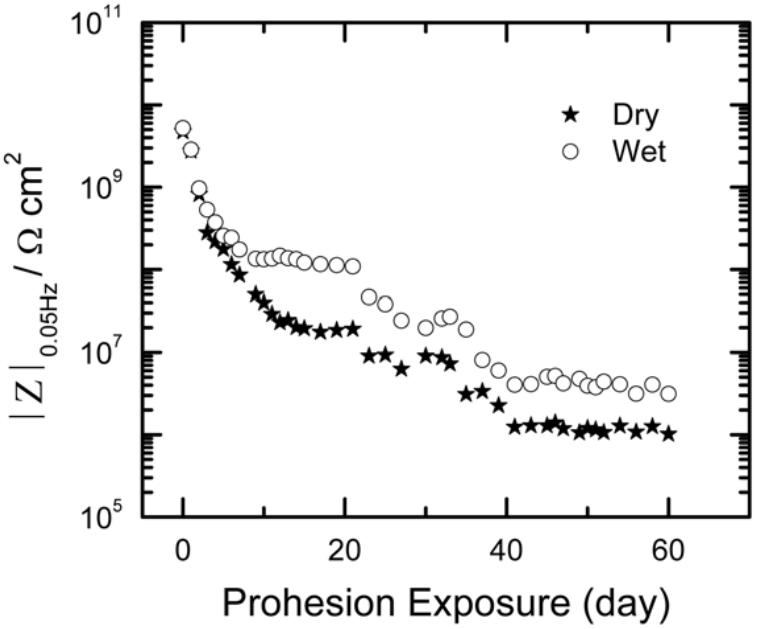

Figure 5. Evolution of the low-frequency impedance $|Z|_{0.05\ Hz}$ values of the 2E sensor-substrate EIS during dry and wet Prohesion steps as a function of time.

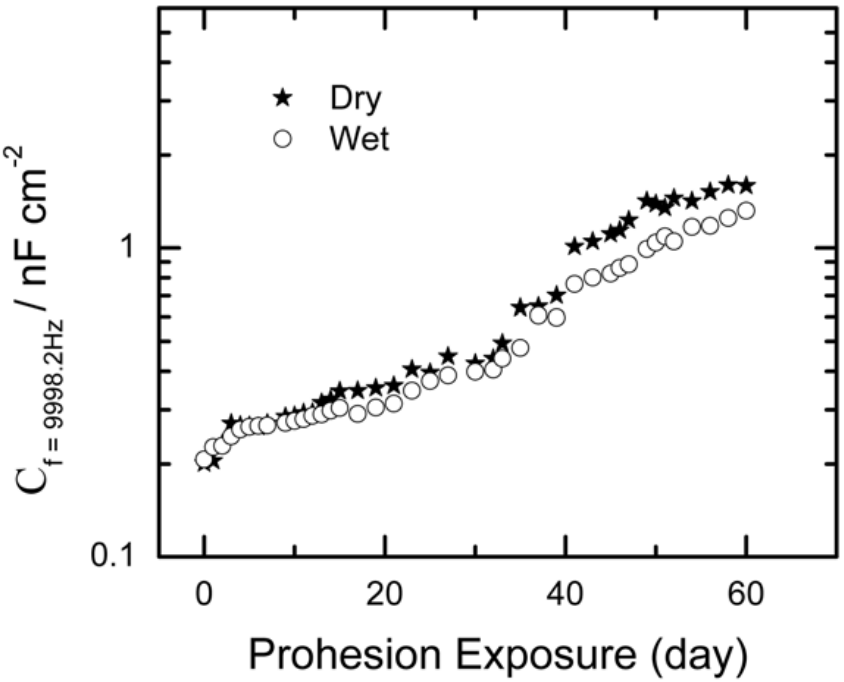

Figure 6. Evolution of the high-frequency capacitance, $C_{9998.2Hz}$, of 2E sensor-substrate EIS during the dry and wet steps of Prohesion as a function of time.

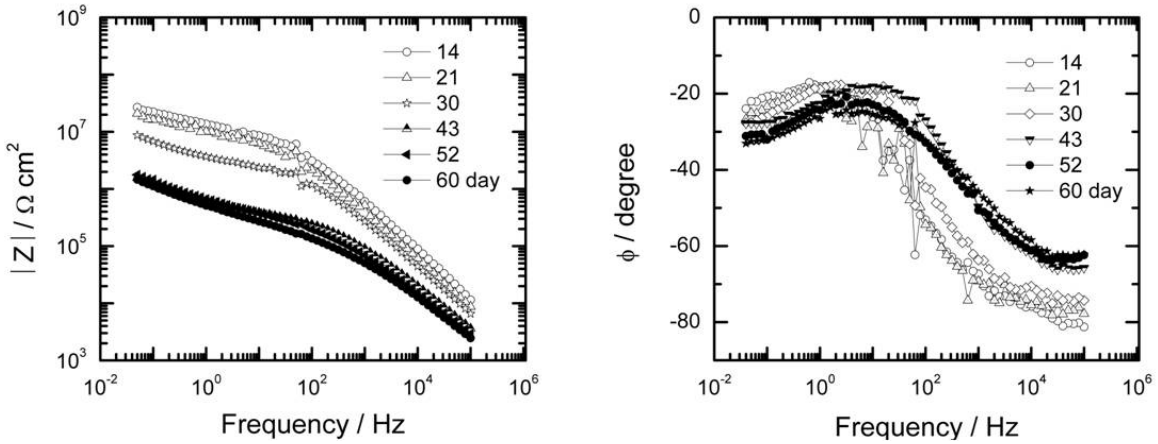

Figure 7. The EIS Bode plots of the coated panel under Prohesion dry step after 40 minutes of drying: (a) impedance modulus, (b) phase angle.

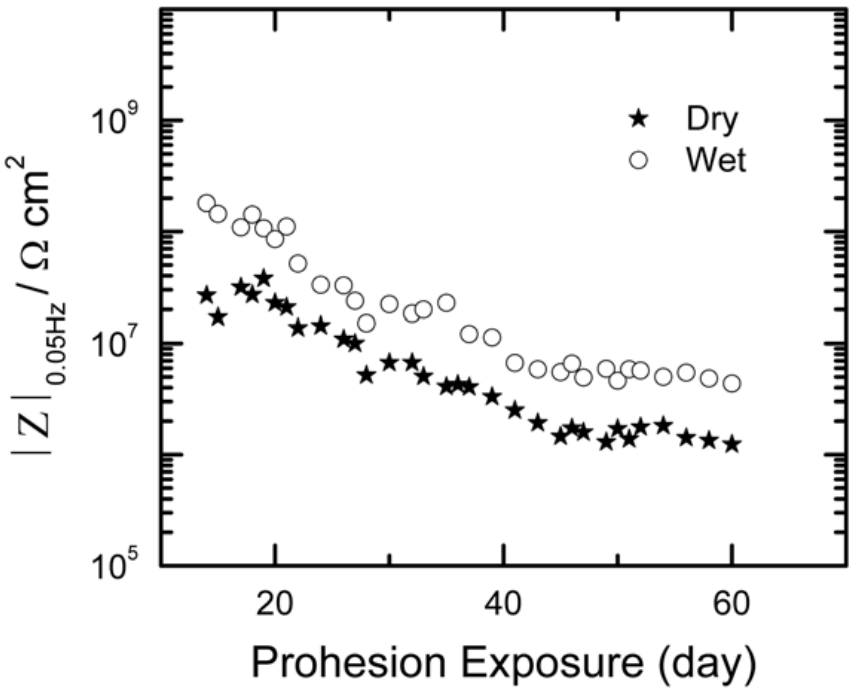

Figure 8. Evolution of the low-frequency impedance $|Z|_{0.05\ Hz}$ values of 2E sensor-sensor EIS during dry and wet Prohesion steps as a function of time.

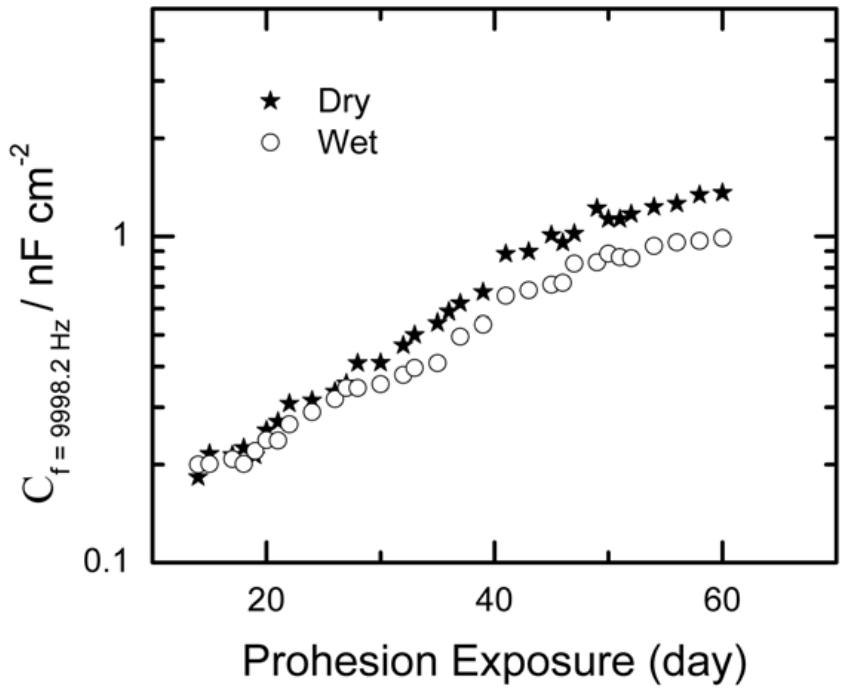

Figure 9. The evolution of the high-frequency capacitance, $C_{9998.2Hz}$, of 2E sensor-sensor EIS during dry and wet Prohesion steps as a function of time.

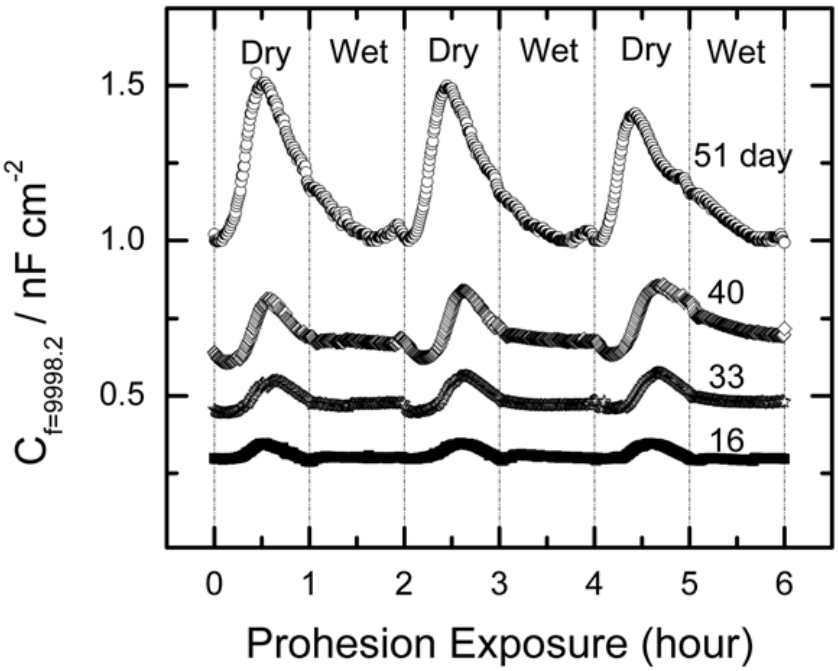

Figure 10. The evolution of high-frequency capacitance, $C_{9998.2Hz}$, during the dry and wet Prohesion steps as a function of time.

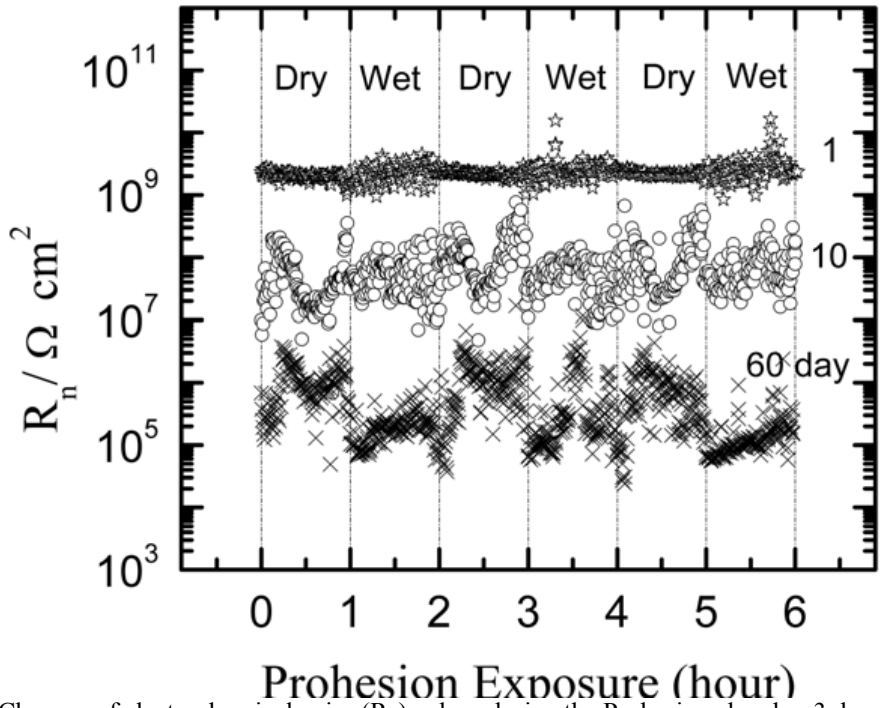

Figure 11. Changes of electrochemical noise (R_n) values during the Prohesion chamber 3 dry and wet cycles at three different exposure times.

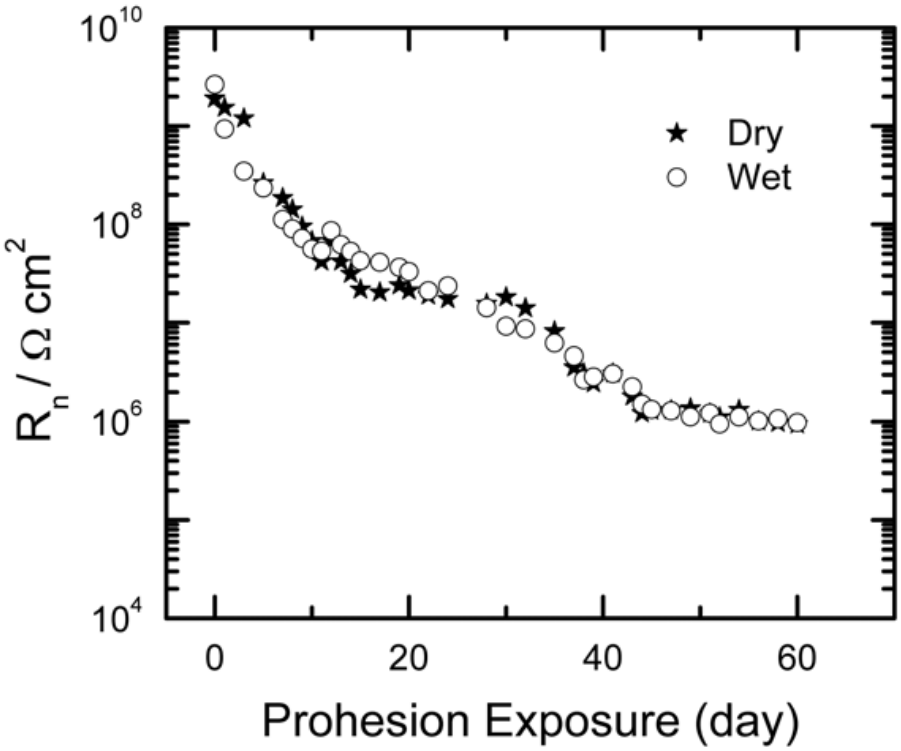

Figure 12. Evolution of the average R_n values obtained from the dry and wet Prohesion steps as a function of time.